ACS OMEGA

http://pubs.acs.org/journal/acsodf

Review

Spiropyran–Merocyanine Based Photochromic Fluorescent Probes: Design, Synthesis, and Applications

Moumi Mandal, Dipanjan Banik, Anirban Karak, Saikat Kumar Manna, and Ajit Kumar Mahapatra*

Cite This: *ACS Omega* 2022, 7, 36988–37007

Read Online

ACCESS | Metrics & More | Article Recommendations

ABSTRACT: Due to ever-increasing insights into their fundamental properties and photochromic behaviors, spiropyran derivatives are still a target of interest for researchers. The interswitching ability of this photochrome between the spiropyran (SP) and merocyanine (MC) isoforms under external stimuli (light, cations, anions, pH etc.) with different spectral properties as well as the protonation–deprotonation of its MC form allows researchers to use it suitably in sensing purposes by developing different colorimetric and fluorometric probes. Selective and sensitive recognition can be achieved by little modification of its SP moiety and functional groups. In this review, we emphasize the recent advancements (from 2019 to 2022) of spiropyran–merocyanine based fluorogenic and chromogenic probes for selective detection of various metal ions, anions, neutral analytes, and pH. We precisely explain their design strategies, sensing mechanisms, and biological and environmental applications. This review may accelerate the improvements in designing more advanced probes with innovative applications in the near future.

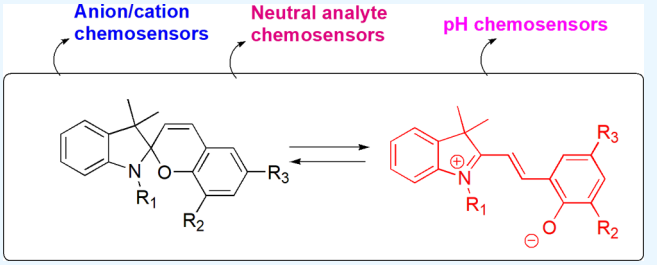

1. INTRODUCTION

Spiropyrans are interesting photoswitches that can undergo reversible structural transformations through isomerization between ring-opened merocyanine (MC) and ring-closed spiropyran (SP) forms (Scheme 1)[1,2] under the influence of stimuli such as stress, light, pH, and thermal effect.[3,4] These two isomers are different in chemical and physical properties such as polarity, molecular volume, color, dipole moment, emission behavior, and net charge,[5] which makes them stand out from other common photoswitches. In 1952, Fischer and Hirshberg reported for the first time the photochromic phenomena and corresponding photochemical reactions of spiropyrans.[6,7]

Scheme 1. Reversible Interconversion between Ring-Closed Spiropyran (SP) and Ring-Opened Merocyanine (MC) Forms

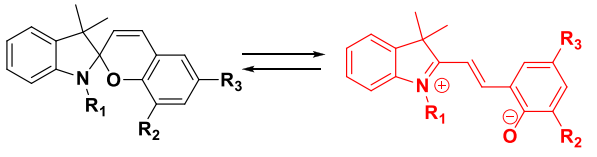

Spiropyrans are well-known with two heteroatomic rings which are structurally linked through a benzopyran moiety connected with indoline through an sp^3 hybridized spiro C atom.[8,9] In spyropyrans, the two rings are perpendicular to each other, which perturbs the delocalization of π-electron conjugation. Thus, the absorption peak appears at 200–400 nm (UV region), resulting in a colorless solid. However, upon irradiation with UV light (200–400 nm), a quick cis–trans isomerization occurs through C–O bond cleavage and results in the formation of a ring-opened intermediate having a zwitterionic benzopyran double bond which contains a positively charged indolium and a phenolate anion, and it is called merocyanine. In ring-opened merocyanine, the two orthogonal heterocyclic moieties gain coplanarity and the molecule turns into an extended conjugated system, which is assisted by a large red shift in the UV–vis (500–600 nm range) for MC compared to SP, resulting in the transformation to a colored species from a colorless form. This process is fully reversible. Upon visible light treatment or heating, the merocyanine form might be converted back to the spiropyran form, obtaining a photochromic system through the ring-closing mechanism.

A salient feature of spiropyran is that the reversible isomerization can be conducted not only by light but also by various other inputs such as solvents, ions, acids and bases, temperature, redox potential, and even mechanical force.[10] In particular, stress as an external stimulus, i.e., a mechanochrom-

Received: August 4, 2022
Accepted: September 26, 2022
Published: October 11, 2022

ism strategy, is broadly used in material applications of spiropyran. By the application of stress, both sides of the spiro center, indoline and chromene moieties, are being pulled apart; that causes the breaking of the C−O bond and, thus, the spiropyran-embedded material changes its molecular shape and goes to the merocyanine form and relieves the strain. Ultrasound and grinding are also included in external stresses. In 2009, Davis et al.[11] reported a force-induced activation of covalent bonds in mechanophore-linked elastomeric and glassy polymers and found that a significant change in color and fluorescence emerged. In 2010, O'Bryan et al.[12] reported stress sensing in polycaprolactone films through an embedded photochromic species by utilizing a difunctional indolinospiropyran as an initiator. In 2012, Wong et al.[13] reported a spiropyran based nanoribbon that reversibly switches its spin polarization by optomechanical stress. Molecular switches from SP to MC are also feasible by changing the temperature in a highly polar solvent or highly acidic condition.

Moreover, substitutions have significant importance for the properties of SPs and their corresponding isomerizations toward different merocyanine derivatives. Different substitutions could be introduced easily at SP fragments through the last synthetic step before spiro carbon is formed. A thorough theoretical study has been performed on the substitution effects of spiropyrans. Brügner et al. fabricated a detailed DFT to predict accurate Hammett parameters, which were being used to investigate the internal energy (ΔU) for SP → MC interconversion for different substitutions on N and carbon atoms.[14] Buncel et al. have reported intense kinetic and mechanistic studies on SP/MC transformations, considering different effects through electron-withdrawing and -donating substituents at the 6-position (C substituent) and the 1′-position (N substituent) and also studied the effects through solvents (solvatochromism) and the pH (acidochromism).[15−17]

The photoswitchable property of spiropyrans has gained huge attention due to the usage of different dynamic chemical systems, such as synthetic polymers, solid surfaces, inorganic nanoparticles, biopolymers, and carbon nanomaterials, having potential biological applications, particularly cell tracking, photothermal therapy labeling, and cell-sheet engineering. Due to interactions with various different materials such as quantum dots (QDs), inorganic metal ions, biologically relevant molecules such as DNA and proteins, and organic systems such as organic small molecules and polymers, it has broad multidirectional application. The photoswitchability of SPs provides many advantages over other colorimetric and fluorescent probes for the detection of organic and inorganic target molecules. For example, by utilizing an external and noninvasive stimulus such as light, the interaction of SPs with the target metal ion can be switched on and off, which extends the sensitivity range and makes it suitable for a wide range of applications, including live cell imaging. In addition, photo-switching of SPs between on and off states at defined times allows one to modulate the sensor signal and correct for a nonmodulated background signal, resulting in high signal-to-noise ratios and a low detection threshold. Lastly, the ability of spiropyran based material to be switched between passive and active states makes it a regenerable detection system with an extended lifetime.

Several reviews on spiropyran based probes have already been published.[18,19] However, because of the widespread interest and quick growth of this issue, the most current research achievements on spiropyran−merocyanine based fluorescent chemosensors must be discussed. As a result, our review properly focuses on and accurately summarizes spiropyran−merocyanine based photochromic fluorescent probes, which are very selective in monitoring metal ions, anions, neutral analytes, and pH, published within the time period from 2019 to 2022, together with their design methods, sensing processes, and applications. We strongly believe that this review will serve as the next generation for the advancement of more potential and exciting spiropyran based fluorescent probes as a molecular detection tool.

2. ANION CHEMOSENSORS

Over the past 25 years, anion sensing has been given more attention because of its role in the fields of biology and industrial processes.[20−22] To meet this need, the design and synthesis of anion sensors to detect environmentally deleterious anions such as cyanide (CN^-) and hypochlorite (OCl^-) have received encouragement from researchers in the areas of supramolecular chemistry and biochemistry. Herein, we provide an overview of different classes of anion sensors (CN^- and OCl^-) based on the spiropyran moiety and highlight the different strategies for sensing toxic anionic species.

2.1. Spiropyran Derivatives as Fluorometric and Colorimetric Probes for Cyanide Ion (CN^-) Detection.

Biological systems are mostly affected by anions, where cyanide is the most toxic and deadly chemical substance.[23,24] Cyanide ions from natural sources and mainly from industrial sources can contaminate water, air, and soil, obstructing cellular respiration and resulting in the death of living organisms. A number of photochromic colorimetric compounds based on the spiropyran moiety were previously reported to detect the exceptionally nucleophilic CN^- anion, monitored through a naked eye color change. By light irradiation, the spiropyran isomerizes reversibly to form an open-ring metastable merocyanine. The CN^- anion addition to a spiro C atom leads to the formation of adduct by the opening of the ring with a distinct color change. Herein, we reported three colorimetric cyanide chemosensors.

In 2014, our research group[25] reported a benzthioimidazole-appended spiropyran probe, **1**, which is selective toward the CN^- anion with a very low detection limit (1.7 mm) in aqueous HEPES buffer solution. The probe was synthesized in three steps. In the first step a condensation reaction was done between salicylaldehyde and *o*-aminothiophenol to produce benzthioimidazole, which was then formylated with hexamine, and the resulting product was used to prepare the targeted probe **1** by reacting it with *N*-2,3,3-tetramethyl indolium cationic salt in ethanol. Mechanistically, the intramolecular charge transfer (ICT) process is being restricted and the fluorescence color has been changed from purple to greenish yellow due to poor electronic conjugation from phenoxide to indolyl cation after CN^- adduct formation (Figure 1). Moreover, probe **1** further recognizes the thiophilic metal Au^{3+} ion against other ions such as Cu^{2+}, Hg^{2+}, and Ag^+. This special characteristic helps the probe to achieve a new feature in logic operations through the properties based on two inputs (i.e., CN^- and Au^{3+}) and the output as the fluorescence response of probe **1**. Additionally, the probe **1** loaded test strip was used as an efficient CN^- test kit in water and it was applied for live cell imaging in RAW 264.7 cells with promising results.

In 2020, Pattaweepaiboon et al.[26] reported a spiropyran derivative, **2**, for quantitative analysis of cyanide ions by a colorimetric method. After isomerization to merocyanine from spiropyran, the CN^- nucleophilic addition toward the spiro

https://doi.org/10.1021/acsomega.2c04969
ACS Omega 2022, 7, 36988−37007

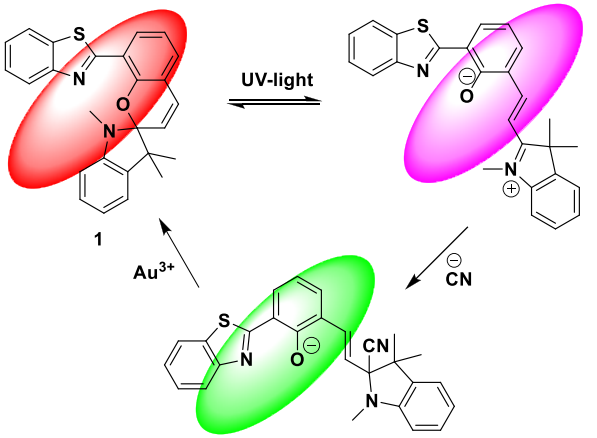

Figure 1. Chemical structure of **1** and its probable sensing mechanism for Au^{3+} and CN^- ions.

carbon atom led to the formation of adduct $[MC-CN]^-$ (Figure2). As a result, the probe color was changed to a vivid yellow from pink, clearly noticed by the naked eye and monitored through UV−visible spectroscopy. Computational analyses and ^1H NMR titration were used to confirm the sensing mechanism. According to a Job plot, probe **2** produced a 1:1 adduct with CN^-, and a binding constant was determined as 8×10^4 M^{-1}. The limit of detection for CN^- was measured to be 0.52 μM. Moreover, a quantitative CN^- analysis, extraction through cassava leaves, was performed with probe **2** in contrast with a standard reference such as Chloramine-T/pyridine-barbituric acid. Paper test strips with this probe were also used to detect CN^- in a portable form.

In 2022, Mahdavian's group[27] for the first time reported two talented colorimetric and optochemical sensors, (*R*/*S*)-2-(3′,3′-dimethyl-6-nitro-3′*H*-spiro[chromene-2,2′-indol]-1′-yl) ethanol (probe **3**) and 9′-hydroxy-1,3,3-trimethylspiro[indoline]-2,3′-[3*H*]naphtho[2,1-*b*][1,4]oxazine (probe **4**), where direct nucleophilic addition of CN^- anion to the closed ring carbon atom of spiropyran ring occurred without any UV irradiation in a 1:1 stoichiometric fashion. After formation of the adduct, a bathochromic shift was noticed, with a distinct color change from colorless to yellow. On the contrary, after UV irradiation and concurrent CN^- addition, **3**-CN and **4**-CN exhibited a color change from violet to yellow to the naked eye. There are two reasons behind these observations. The first one is that the two electronegative atoms, nitrogen and oxygen, are directly linked to the spiro carbon, which enables the probe to be more electron deficient than that product. The second one is that, after the formation of an adduct, the phenoxide group is conjugated with the newly formed alkene group. The affinity of these two probes toward the CN^- in the presence of other analytes is presented in Figure 3. The detection limits of **3** (0.091 μM, 2.36 ppb) and **4** (0.094 μM, 2.44 ppb) sensors toward CN^- were lower than the WHO's permitted level in drinking water (1.9 μM).

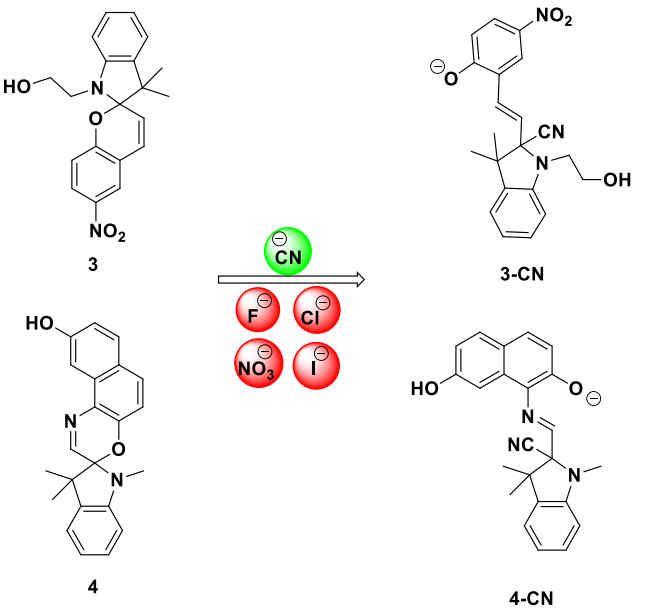

Figure 3. Selective reactivity of **3** and **4** toward CN^- in the presence of other competitive anions.

2.2. Spiropyran Derivatives as Fluorescent Probes for the Hypochlorite (OCl^-) Ion. Among all other reactive oxygen species (ROS), hypochlorous acid (HClO) is a well-known ROS because of its diverse usage in the immune system and is commonly used as a bleaching agent,[28,29] but too much hypochlorite can cause severe oxidative damage in a living body, which could lead to a number of immune-related diseases and disorders such as osteoarthritis, rheumatoid arthritis, atherosclerosis, cardiovascular diseases, and malignancies.[30,31] Thus, the highly selective and sensitive quantification of ClO^- is actively anticipated in recent research. This section will discuss a spiropyran based hypochlorite chemosensor.

In 2019, Samanta et al.[32] designed a cyanine based fluorogenic probe, **5**, which exhibits turn-on fluorescence particularly in mixed aqueous medium toward hypochlorite. The probe was prepared by the reaction between the iodide salt of 3-ethyl-1,1,2-trimethyl-1*H*-benzo[*e*]indol-3-ium and 2-hydroxy-1-naphthaldehyde in the presence of anhydrous sodium acetate in ethanol. According to the report, probe **5** can show solvent polarity-induced distinct isomerization. Initially, the probe is non-

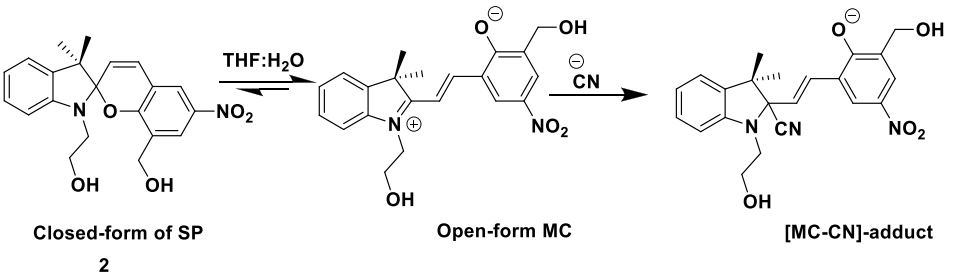

Figure 2. Chemical structure of **2** and its detection mechanism for CN^- ion.

https://doi.org/10.1021/acsomega.2c04969
ACS Omega 2022, 7, 36988−37007

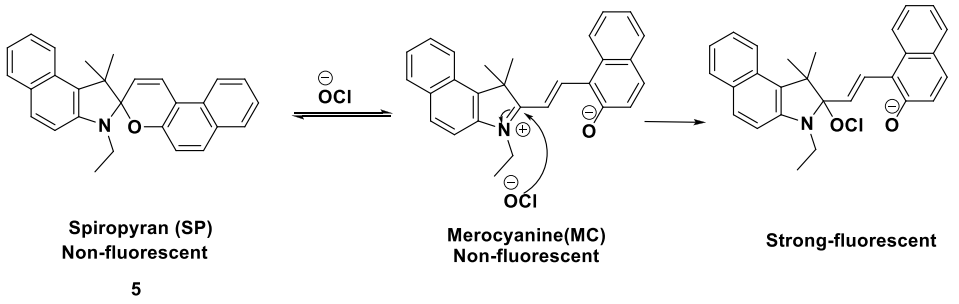

Figure 4. Plausible sensing mechanism of probe **5** with hypochlorite.

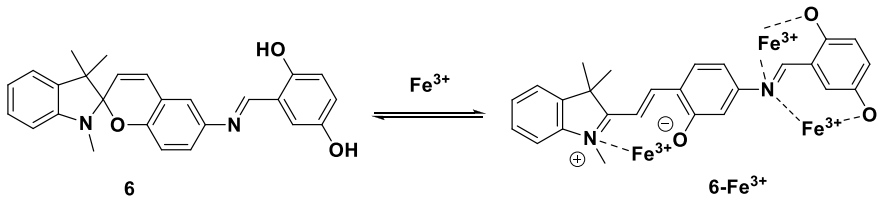

Figure 5. Probable mode of complexation of probe **6** with Fe^{3+}.

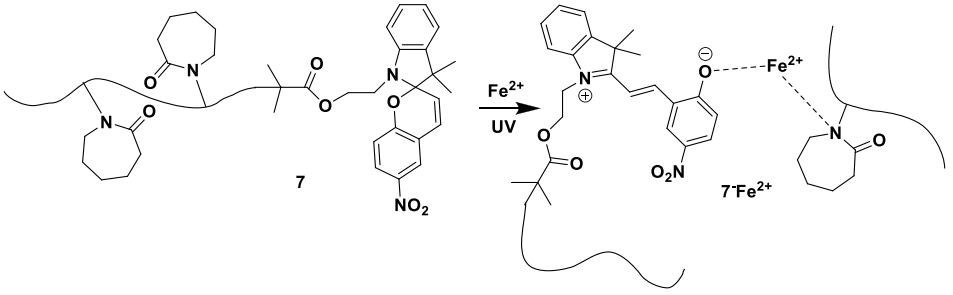

Figure 6. Coordination mechanism of probe **7** in the presence of Fe^{2+} under UV irradiation.

fluorescent where its merocyanine (MC) form is predominant, but after nucleophilic addition of OCl^-, there is an occurrence of 10-fold enhancement of fluorescence intensity at 435 nm owing to the formation of an OCl^- adduct which disrupts donor−acceptor extended π-conjugation. Therefore, decolorization from violet to colorless of the solution of probe **5** was observed with the naked eye. The probe shows a strong absorption peak at 583 nm due to its $\pi-\pi^*$ charge transfer of the conjugated cyanine moiety in its MC form. The detection limit was found to be 3 μM. The proposed sensing method is depicted in Figure 4.

3. CATION CHEMOSENSORS

Metal ions such as Cu^{2+}, Fe^{3+}, and Li^+ play crucial roles in copious biological processes. But they are extremely poisonous if they exceed the limit of tolerance value suggested by the WHO. Therefore, in recent years, researchers have been attracted to molecular design for the detection of cations with its potential applications and environmental monitoring.[33,34] However, heavy metal ions such as Hg^{2+} and Pb^{2+} are great threats to living organisms because they are highly toxic, nondegradable environmental pollutants. Therefore, the detection of these ions is gaining popularity in the field of supramolecular chemistry. In this section we report various chemosensors for Fe^{3+}/Fe^{2+}, Cu^{2+}, Hg^{2+}, Cr^{3+}, Ce^{3+}, Ca^{2+}, Pb^{2+}, and Li^+ ions.

3.1. Spiropyran Derivatives as Colorimetric and Fluorescent Probes for Fe^{3+}/Fe^{2+}. Iron plays a vital role in numerous biological activities such as cellular metabolism, oxygen carrying, enzymatic reaction, and various biosyntheses.[35] However, an excessive amount of iron can lead to various diseases such as osteoporosis, heart disease, liver and kidney damages, Alzheimer's disease, and even cancer. Again, a deficiency of iron is also harmful and can cause anemia. Therefore, effective detection of iron is gaining in importance in different areas of research. Recently, a number of spiropyran based fluorescent probes have been developed for the detection of Fe^{3+}/Fe^{2+}.

In 2019, Zhang et al.[36] designed and synthesized a multiple phenolic −OH group based spiropyran probe, **6**, for the selective recognition of Fe^{3+} in both organic and aqueous media. It was obtained by a three-step reaction starting with 1,2,3,3-tetramethylindolindolenium iodide and 5-nitrosalicylaldehyde. Probe **6** is able to detect Fe^{3+} in a wide range of pH varying from 4.5 to 10.5 and exhibits a low detection limit of 1.93×10^{-7} M. From a Job plot, it was found that the stoichiometric ratio of the probe and the Fe^{3+} ion is 1:3. This ratio can be explained as the binding of two Fe^{3+} ions with two −OH groups and one Fe^{3+} with the ring-opened form of the probe (Figure 5). This complexation was the reason for the 50-fold enhancement in fluorescence intensity at 450 nm.

Yang et al.[37] designed and synthesized the spiropyran-ended polymer **7** by a technique of atom transfer radical polymerization. They used *N*-vinyl caprolactam (NVCL) as a monomer to construct polymer **7** as it is biocompatible and environmentally friendly; additionally, the amino groups present in its

https://doi.org/10.1021/acsomega.2c04969
ACS Omega 2022, 7, 36988−37007

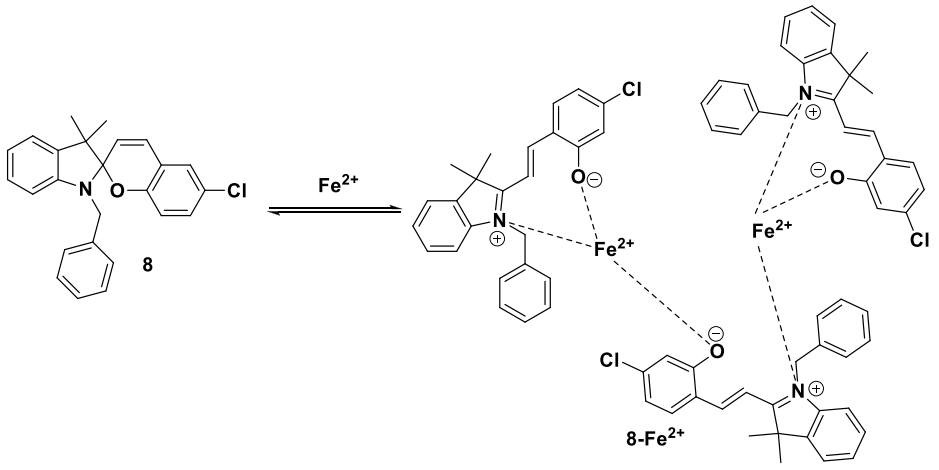

Figure 7. Plausible sensing mechanism of probe **8** with Fe^{2+}.

structure can help in coordination with metal ions. Probe **7** was successfully employed in the recognition of Fe^{2+}. Probe **7** in THF solution exhibited no absorption peaks above 400 nm in the absence of UV light irradiation, but after irradiation, absorption at 591 nm was observed with a conversion of solution color from colorless to pink. This outcome was attributed to the probe's transformation from its ring-closing form to its ring-opening form under UV irradiation, as seen in Figure 6. Thereon, this coordination resulted an obvious color change to the naked eye with generation of the absorbance peak at 438 nm. The limit of detection of the polymeric compound **7** for Fe^{2+} was also calculated as 0.00298 mM.

In 2021, Cong's group[38] reported a spiropyran fluorescent probe **8**, which was synthesized by a two-step reaction (in the first step N-alkylation of 2,3,3-trimethyl-3*H*-indole with benzyl bromide was done, and in the second step a condensation reaction was done with the intermediate *N*-benzyl-2,3,3-trimethyl-3*H*-indolium bromide and 5-chlorosalicylaldehyde) for dual recognition of Fe^{2+} and pH. Probe **8** in 9:1 EtOH/H_2O exhibited weak fluorescence, but in the presence of Fe^{2+}, a 6-fold enhancement in fluorescence intensity at 360 nm was found. This enhancement in fluorescence was due to the complex formation, and interestingly the stoichiometric ratio of the probe and Fe^{2+} was 3:2 in that complex (Figure 7). Furthermore, probe **8** responds interestingly in different pHs. In acidic pH the probe shows a colorimetric change: the color of the solution changes from colorless to yellow at pH 1−2. On the other hand, in alkaline pH the probe responds in a fluorometric way: the probe shows weak emission at 360 nm in pH <13, but at pH 14 the fluorescence emission increases at 360 nm with the emergence of a new peak at 430 nm.

3.2. Spiropyran Derivatives as Fluorescent Probes for Cu^{2+}. Copper(II) is a common element and is crucial for the development, growth, and fitness of living organisms.[39] However, a of deficiency Cu^{2+} or excessive Cu^{2+} in the living body may cause various health issues because Cu^{2+} has good redox properties, which are responsible for the production of reactive oxygen species (ROS).[40,41] Therefore, researchers have been attracted to developing a selective, sensitive, cost-effective fluorescent probe for the sensing of Cu^{2+} ions. There are several reports regarding the use of spiropyran based fluorescent probes for selective detection of this metal ion. Three spiropyran based chemosensors for the recognition of Cu^{2+} ions are discussed in detail in this section.

Kumar's group[42] designed and synthesized the benzothiazolinic spiropyran **9** (Figure 8) possessing a methoxy group at the

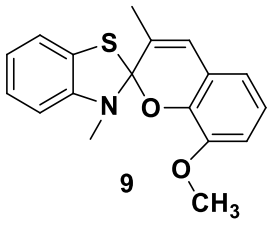

Figure 8. Structure of probe **9**.

ortho position to the phenolic oxygen atom for better accommodation of the metal ion. It was synthesized by the reaction between *o*-vanillin and [*E*]-2-ethylidene-3-methyl-2,3-dihydrobenzo[*d*]thiazole in ethanol. The probe can recognize Cu^{2+} in a reversible manner. The probe in aqueous acetonitrile solvent showed an absorption band in the wavelength region of 280−330 nm. Upon the addition of 1 equiv of Cu^{2+}, the absorption band was shifted to the 430−570 nm region with the highest absorption at 500 nm, whereas no change in absorption was found in the presence of other comparative metal ions. A Job plot analysis predicted a 1:1 binding stoichiometry between the probe and Cu^{2+} ions. The limit of detection of probe **9** was found to be 0.75 μM.

In 2020, Xuan et al.[43] reported a spiropyran fluorescent probe, **10** (Figure 9), for heating-promoted sensing of Cu^{2+}. It was obtained by a two-step reaction: in the first step 1-ethyl-2,3,3′-trimethyl-3*H*-indolium iodide was produced; this product was further reacted with 2-hydroxy-5-nitrobenzaldehyde to generate the probe. Probe **10** solution in the presence of Cu^{2+} did not show any emission peak at 568 nm at room temperature (20 °C), but with an increase in temperature from 20 to 30 °C the emission peak grew to 568 nm. No absorption peak was generated at this temperature. After the temperature of 50 °C was reached, strong emission and absorption peaks arose at 568 and 550 nm, respectively. The probe was opened up under UV irradiation, and in the presence of Cu^{2+} in DMF solution, a ternary complexation occurred. The ring-opened form exhibited a distinct fluorescence color from the probe−Cu^{2+} complex, which had brighter fluorescence than the previous one under the illumination of a laser pointer.

https://doi.org/10.1021/acsomega.2c04969
ACS Omega 2022, 7, 36988−37007

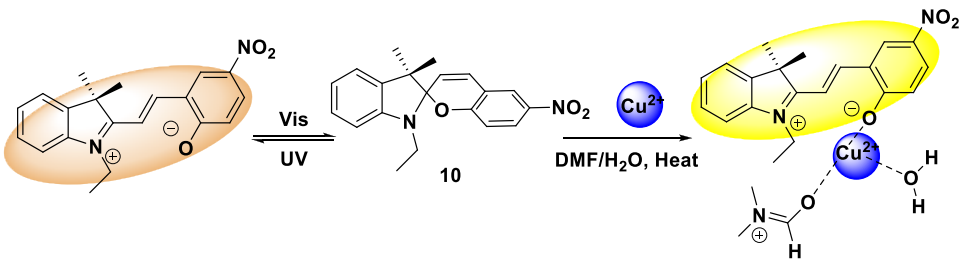

Figure 9. Structure of probe **10** and its probable sensing mechanism.

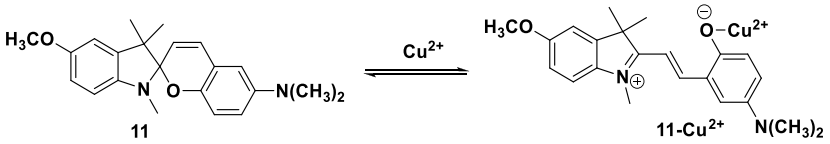

Figure 10. Mode of binding of probe **11** with Cu^{2+}.

In 2021, Louie's group[44] designed and synthesized the dimethylamine-functionalized spiropyran **11** (Figure 10) by a condensation reaction between indolium iodide and dimethylaminobenzaldehyde for the colorimetric detection of Cu^{2+}. The authors suggested that the presence of electron-donating diethylamine substituents reduced the conversion of the spiro form to the mero form, resulting in large absorption bands at 250 and 312 nm, which corresponds to the spiro form. But upon UV irradiation, an enhanced absorption band was observed at 483 nm, indicating the conversion to the mero form of **11**. Again, upon addition of 1 equiv of Cu^{2+} strong absorbance appeared at 418 and 667 nm. A hypsochromic shift from 483 to 418 nm was attributed to the local environment in the presence of copper salt, and a new absorbance at 667 nm was attributed to the complex formation between the mero form of **11** and Cu^{2+}. From a Job plot, the author proved that the stoichiometric ratio of the probe and Cu^{2+} in the complex was 1:1, and the detection limit was found to be as low as 0.11 μM.

3.3. Spiropyran Derivatives as Fluorescent Probes for Hg^{2+}. Mercury(II) is one of the most harmful heavy metal ions and can be associated with carboxyl, thiol, and phosphate in biological bodies, leading to serious health problems.[45] Therefore, the demand for simple and efficient Hg^{2+} detection remains. Among various analytical methods, the fluorescence chemosensor method is gaining importance due to its simplicity.

Kumar et al.[46] designed and synthesized a spiropyran fluorescent probe, **12** (Figure 11), by introducing a methoxy group to the ortho position of the phenolic oxygen atom, and it was obtained by the reaction between 2-hydroxy-3-methoxy-5-nitrobenzaldehyde and 2-ethyl-3-methylbenzo[*d*]thiazol-3-ium-4-toluenesulfonate in the presence of piperidine. Probe **12** in CH_3CN/water (1:1) can detect Hg^{2+} by complex formation, resulting in changes in both colorimetric and fluorometric responses. Interestingly, probe **12** forms a complex with Hg^{2+} in the absence of UV light (365 nm, 3 W), but it reverts to its spiropyran form in the presence of light. Three detection limit values (5.5 μM, 78.5 nM, and 0.62 μM) were calculated with the use of three different methods (UV−vis spectroscopy, fluorescence spectroscopy, and digital image analysis). Digital image analysis gives better results in the detection limit value compared to UV−vis spectroscopy. Further, the practical applicability of the probe was shown in a filter paper strip detection method.

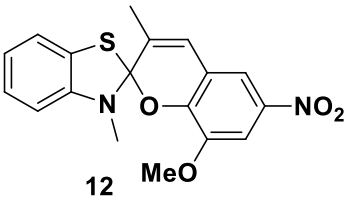

Figure 11. Structure of probe **12**.

3.4. Spiropyran Derivatives as Fluorescent Probes for Ce^{3+}. In recent years, the electroluminescence of lanthanide ions has created continuous curiosity as potential light-emitting materials in light-emitting diodes (LEDs). Being a member of the lanthanide ions, Ce^{3+} possesses the special ability of parity-allowed electric-dipole 4f → 5d transitions, which results in high light outputs.[47] Therefore, the detection of Ce^{3+} ion is a promising one in research. In this section, an example of a Ce^{3+} chemosensor is presented.

Luo et al.[48] reported a probe, **13** Figure 12, for selective sensing of Ce^{3+} in EtOH/H_2O (9:1 or 1:9, v/v) media. It was synthesized through the condensation reaction between a quaternary ammonium salt and 3-methoxysalicylaldehyde. Free probe **13** in an EtOH/H_2O (9:1, v/v) solvent system exhibited weak emission at around 350 nm, but upon gradual addition of Ce^{3+} the emission band was increased with slight shifting to a higher wavelength of 360−380 nm. This change in emission was attributed to the 1:1 complexation between the probe and Ce^{3+}. A selectivity test was performed with other competing metal cations (Li^+, Na^+, Ag^+, Sr^{2+}, Ni^{2+}, Co^{2+}, Hg^{2+}, Cu^{2+}, Zn^{2+}, Cr^{3+}, Al^{3+}, Nd^{3+}, Yb^{3+}, La^{3+}, Fe^{3+}, Bi^{3+}, 1 equiv), but these ions could not change the emission property of probe **13**. Therefore, the probe was selective toward Ce^{3+} and the detection limit was found to be 1.7 μmol/L. Moreover, the

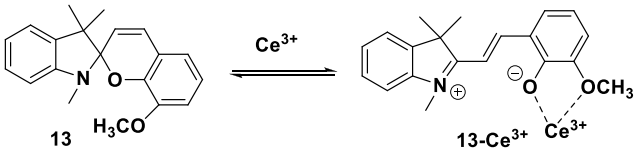

Figure 12. Probable mode of binding of probe **13** with Ce^{3+}.

https://doi.org/10.1021/acsomega.2c04969
ACS Omega 2022, 7, 36988−37007

probe was practically applied for the detection of Ce^{3+} in real water samples.

3.5. Spiropyran Derivatives as Colorimetric Probes for Cr^{3+}. Chromium(III) is one of the effective trace nutrients that have control over human metabolism and diet by regulating the glucose tolerance factors and insulin action. In the human body, for a balanced diet, an adequate intake of Cr^{3+} is 25−200 μg/day. Overload or deficiency of Cr^{3+} may cause adverse health effects such as cardiovascular diseases, diabetes, and neurological disorders.[49] This section discusses the Cr^{3+} chemosensor.

By using nitrosalicylaldehyde, Gao's group[50] developed a spiropyran probe, **14** (Figure 13), which can recognize Cr^{3+} in

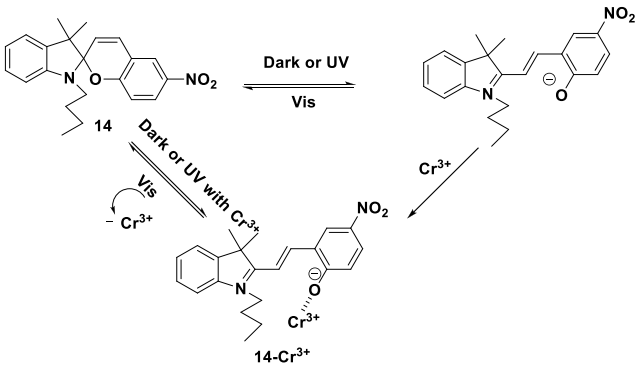

Figure 13. Plausible sensing mechanism of probe **14** for Cr^{3+}.

an interesting manner of negative photochromism. This negative photochromism implies the detection of Cr^{3+} by the probe without UV irradiation. Under this condition, the color of the probe solution in MeOH/H_2O (9:1, v/v) was changed, which was attributed to the complex formation between the MC form of **14** and Cr^{3+}. The binding constant and detection limit of the probe were estimated, and they were 8.7×10^3 M^{-1} and 0.64 μM, respectively. Again, inspired by the various advantages of hydrogels such as good biocompatibility, nontoxicity, hydrophilicity, low cost, porous structure, and portability, this group prepared the hydrogel of probe **14** to engage it as a functional material for reversible adsorption and desorption on Cr^{3+} in mixed solution.

3.6. Spiropyran Derivatives as Fluorescent Probes for Ca^{2+}. Calcium ions play a crucial role in the human body, and calcium is a very important element of bone and teeth. However, this ion also participates in the transmembrane transport of biological information and modifies the response of cells to external stimuli. However, calcium ion deficiency can cause a variety of health issues, including osteoporosis, growth retardation, and hypertension.[51] Therefore, an easy and effective method for the detection of Ca^{2+} has a great impact.

Wang's group[52] constructed a spiropyran probe, **15** (Figure 14), to recognize the Ca^{2+} ion through a "turn-on" response. An electron-withdrawing cyano group was introduced in the probe to facilitate isomerization by weakening the C−O bond of the closed SP form. It was obtained by a three-step reaction: in the first and second steps 5-cyanosalicylaldehyde and 1-(2-carboxyethyl)-2,3,3-trimethyl-3*H*-indolium bromide were produced, respectively, and then these two were reacted to give probe **15**. To avoid the photoisomerization between SP and MC forms of probe **15**, absorption and fluorescence spectra were recorded in two different photoexcitations (375 and 290 nm). Depending on the results, the authors chose the photoexcitation of 375 nm and succeeded in avoiding photoisomerization. In absorption, probe **15** exhibited four absorption bands at 236, 287, 357, and 414 nm, but upon incremental addition of Ca^{2+}, a new absorption band at 526 nm appeared with decreases in absorption at 357 and 414 nm. This result was attributed to Ca^{2+} promoted ring opening to form MC. Again, in fluorescence spectra, a continuous enhancement in emission at 604 nm was observed with the gradual addition of Ca^{2+}. From a Job plot it was shown that 1:1 complex formation occurs between probe **15** and Ca^{2+}. The association constant and limit of detection were determined to be 2.47×10^3 M^{-1} and 4.53×10^{-8} M, respectively.

3.7. Spiropyran Derivatives as Fluorescent Probes for Pb^{2+}. Being one of the heavy metal ions, Pb^{2+} has received significant attention due to its essential role in various fields and its high toxicity. Excessive intake of this ion may lead to muscle paralysis, mental retardation, and memory loss, particularly in children.[53] Therefore, an effective platform is required for the recognition of Pb^{2+}.

Lin and co-workers[54] reported **16** as an aggregation induced emission (AIE) based fluorescent probe containing a tetraphenylethene (TPE) unit linked with a merocyanine unit for selective detection of Pb^{2+} in THF/H_2O (1:9, v/v) by a FRET-off mechanism (FRET, Förster resonance electron transfer; Figure 15). The bifluorophoric nature of probe **16** was explained astonishingly by its linking structure. The probe contains two units: the donor TPE unit and the acceptor MC unit, of which the former is responsible for blue emission and the latter is responsible for red emission. In the UV exposure (at 365), the open MC form of **16** predominates; as a consequence, a rise in the emission at 635 nm was noticed due to the FRET process. Upon gradual addition of Pb^{2+}, coordination occurs between the probe and Pb^{2+}, FRET becomes off, and, as a result, the emission at 480 nm gradually increases with a gradual decrease of emission at 635 nm. Moreover, probe **16** was successfully applied for live cell imaging in HeLa cells with more than 80% cell viability up to 25 μM probe concentration and a better detection limit of 0.27 μM was found as an AIE sensor.

In 2022, Liu et al.[55] designed and synthesized compound **17** for selective, visual detection of Pb^{2+}. It was synthesized by the

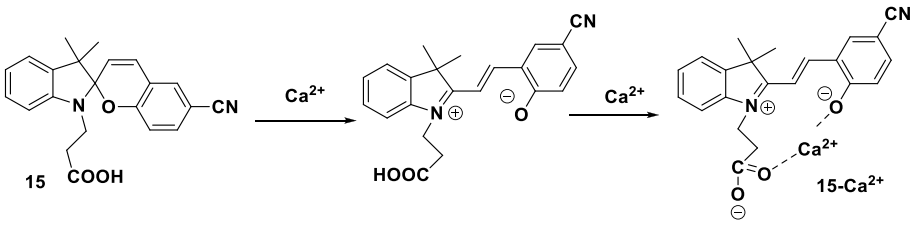

Figure 14. Plausible mode of sensing of probe **15** with Ca^{2+}.

https://doi.org/10.1021/acsomega.2c04969
ACS Omega 2022, 7, 36988−37007

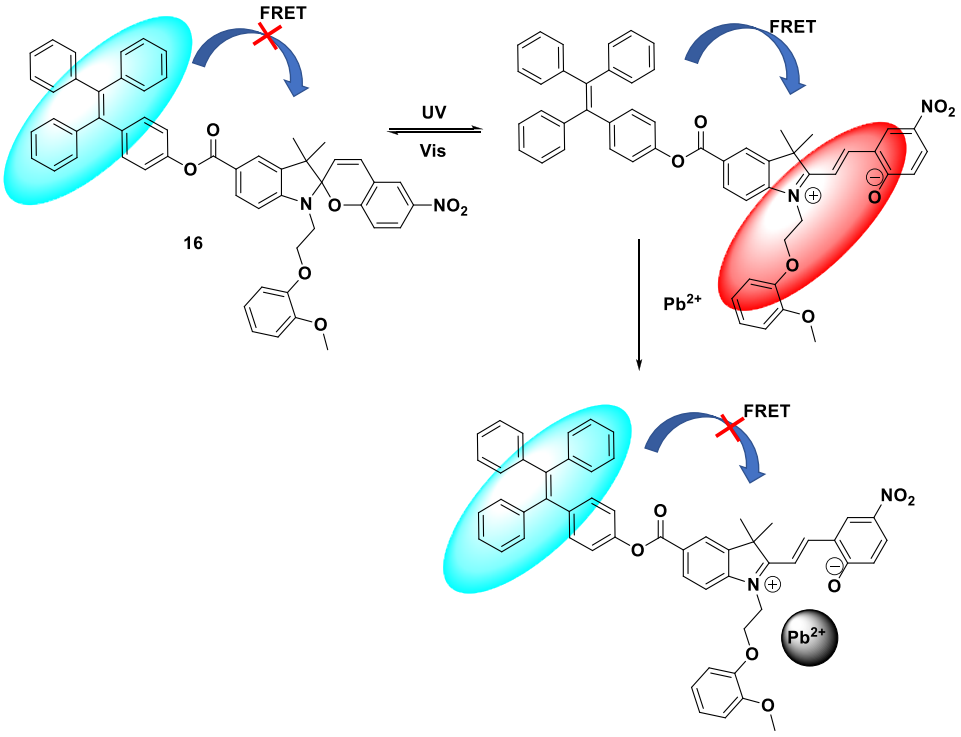

Figure 15. Possible sensing mechanism of probe **16** with Pb^{2+}.

reaction between 1-(4′-carboxybutyl)-2,3,3-tetramethyl-3*H*-indoline bromide salt and 2,3-dihydroxy-5-nitrobenzaldehyde. The probe exhibited wonderful solvatochromism in polar solvent due to the presence of hydroxyl groups (participating in hydrogen bonding) in the 8-position of the pyran ring. In visible light conditions, probe **17** can isomerize to its open MC form, which upon addition of Pb^{2+} readily forms a complex in a 1:1 stoichiometric manner. Therefore, a change in color of the probe solution was observed. There is no requirement for UV irradiation for lead recognition because the complex is remarkably stable under visible light. This stability was considered to be induced by the interaction of Pb^{2+} with the deprotonated carboxyl group, phenolic oxygen atom, and 8-hydroxyl group, as illustrated in Figure 16. The limit of detection and binding constant were determined to be 0.61 μM and 1.37×10^4 M^{-1}, respectively.

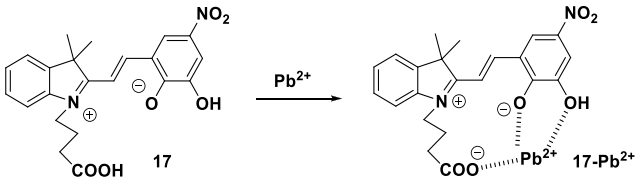

Figure 16. Probable binding mode of probe **17** with Pb^{2+}.

3.8. Spiropyran Derivatives as Fluorescent Probes for Li^+. Lithium salts, especially lithium carbonate, have great uses in the treatment of bipolar disorders and also in dementia-related health issues. But it is difficult to determine the correct dose for every patient since the effective amount of lithium diversely depends on an individual's metabolism and other variables. Exposure to excessive lithium can damage the nervous system and kidneys permanently.[56] Therefore, easy and effective recognition of Li^+ ions is needed.

Kang et al. synthesized a spiropyran derivative, **18**, by introducing aza-12-crown-4 unit as a recognition site for Li^+ ion.[57] It was synthesized by a three-step reaction: by a two-step reaction an intermediate was generated and this intermediate was reacted in the third step with monoaza-12-crown-4 in DMF. Due to the presence of the crown moiety the complexation ability of the probe increases, and in the presence of Li^+ the SP form of the probe converts into the MC form, producing **18**−Li^+ complex (Figure 17). This complex formation was supported by ESI-MS spectra. Owing to complex formation, an increase in the absorption was observed between 450 and 600 nm and also an enhancement in the fluorescence was found. Again, a selectivity study was performed with **18** in the presence of other similar kinds of metal ions such as Na^+, K^+, Ca^{2+}, Mg^{2+}, Cu^{2+}, Zn^{2+}, Fe^{2+}, and Hg^{2+}, but no changes were found in the occupancy of these ions. Furthermore, live cell imaging was performed in Hela cells and in vivo imaging was done in zebrafish with a good turn-on fluorescence response.

3.9. Spiropyran Derivatives as Fluorescent Probes for Multiple Ions. Some compounds may recognize more than one ion and be regarded as multiple ion chemosensors. Recently, a spiropyran based chemosensor has been reported which can detect many cations simultaneously.

Meng's group[58] reported a spirobenzopyran based compound, **19**, for multiple ion detection. Probe **19** can recognize Hg^{2+}, Cu^{2+}, Ce^{3+}, Cr^{3+}, and Al^{3+} in the naked eye and also in the fluorescence method. However, limits of detection were calculated only for Cu^{2+} and Hg^{2+} ions, and they were 10 and 14 μM, respectively. From a Job plot, the authors showed that the stoichiometric ratio in the complex of probe **19** and Cu^{2+} was 2:1, and the mode of binding is presented in Figure 18.

https://doi.org/10.1021/acsomega.2c04969
ACS Omega 2022, 7, 36988−37007

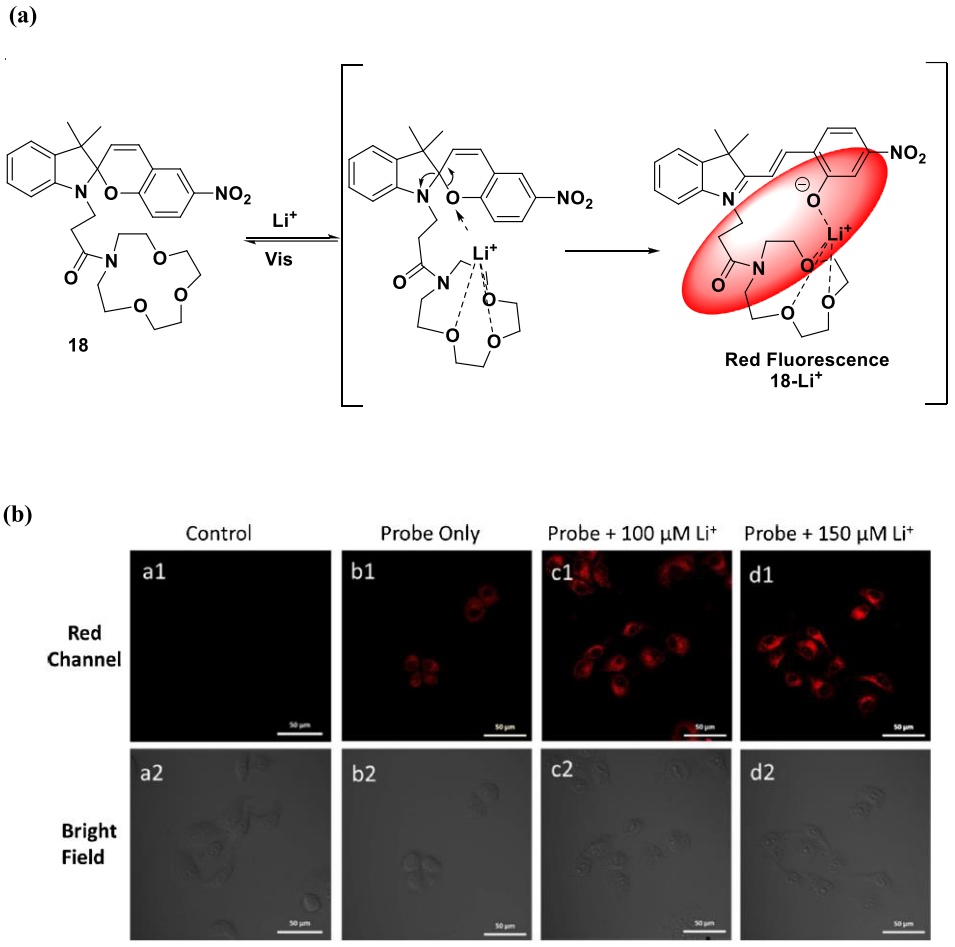

Figure 17. (a) Plausible binding mode of probe **18** with Li^+. (b) CLSM images of HeLa cells. Reprinted with permission from ref 57. Copyright 2021 Elsevier.

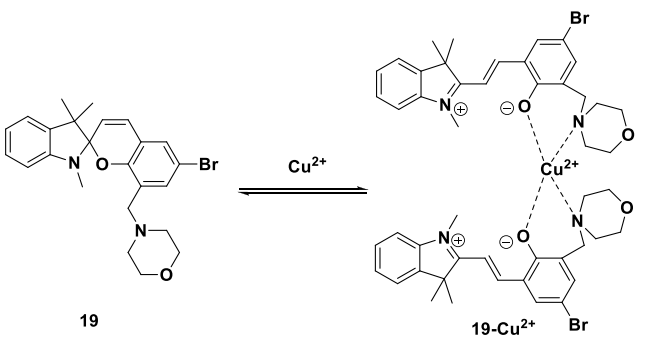

Figure 18. Probable binding mode of probe **19** with Cu^{2+}.

4. FLUORESCENT CHEMOSENSORS FOR NEUTRAL ANALYTES

Small neutral analytes, in addition to anions and cations, are crucial for a variety of pathological and physiological functions. For the detection of small neutral analytes, a number of fluorescent probes based on various design approaches have been published.[59] In this section, we will discuss a few spiropyran−merocyanine based chemosensors for small neutral analytes, such as PhSH, H_2S, and amine, along with their design approaches, sensing processes, and applications.

4.1. Spiropyran Derivatives as Fluorescent Probes for Thiophenol (PhSH). Among a class of highly reactive and toxic aromatic thiols, thiophenols are the most important toxic raw materials for the environment. In addition, they have widespread

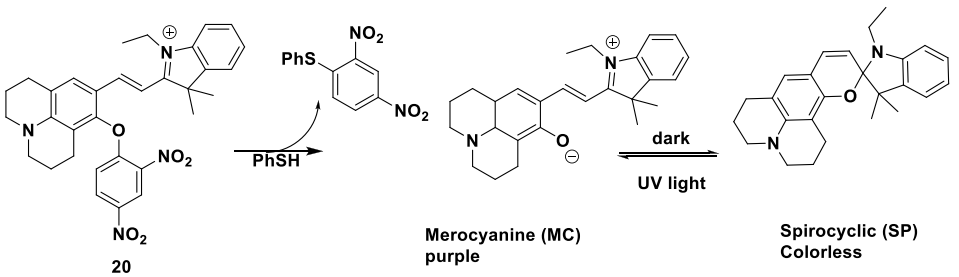

Figure 19. Probable sensing mechanism of probe **20** for PhSH.

https://doi.org/10.1021/acsomega.2c04969
ACS Omega 2022, 7, 36988−37007

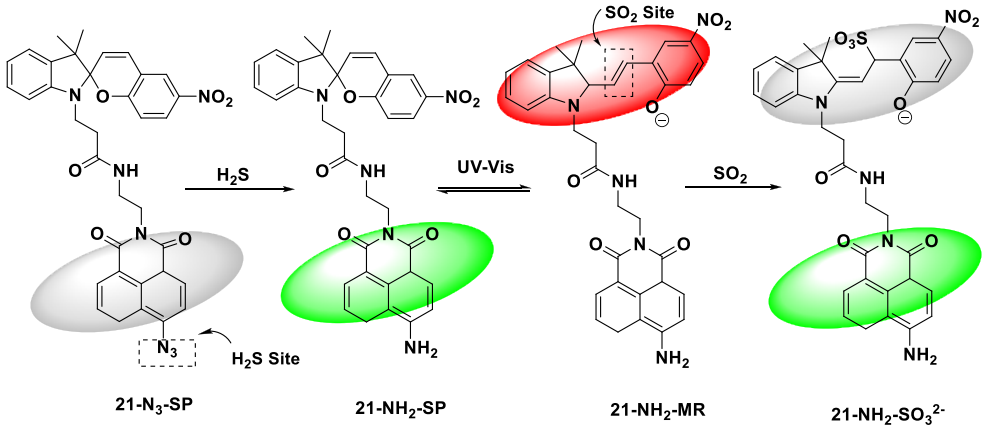

Figure 20. Proposed sensing mechanism of probe **21** for H_2S and SO_2.

uses in the chemical industry for the preparation of different polymers, pesticides, and medicines.[60,61] Therefore, thiophenols are marked as pollutants by the U.S. Environmental Protection Agency. Long-term thiophenol exposure produces significant health problems such as expiratory dyspnea, central nervous system damage, and even death.[62−64] Therefore, designing a selective method for the detection of thiophenols is of great importance nowadays.

In 2007, Wang et al., first reported a benzoxazole based fluorescence probe to detect thiophenols.[65] Later on, in 2019, Yang et al.[66] reported a 2,4-dinitrobenzenesulfonamide based fluorometric and colorimetric probe, **20** (Figure 19), for the detection of thiophenol through the nucleophilic substitution−cyclization reaction. Upon the addition of thiophenol, the highly electron-withdrawing capacity of the 2,4-dinitrobenzenesulfonamide unit was cleaved. As a result, the probe went to its merocyanine form, which was further rapidly isomerized to the closed spiropyran form and leading to the purple color of the solution being changed to colorless to the naked eye. This is because of the ICT process, and the extended π-conjugation of the merocyanine moiety was disrupted. The probe responded quickly (within 30 s) and had a high sensitivity (detection limit of 0.55 M) to thiophenols in the presence of other sulfur species. Furthermore, probe **20** precisely measures thiophenols in water samples, revealing a unique and potential method of thiophenol detection.

4.2. Spiropyran Derivative as Fluorescent Probe for H_2S/SO_2 Dual Sensing. Among all reactive sulfur species (RSS), hydrogen sulfide (H_2S) and sulfur dioxide (SO_2) have been the best-known air pollutants for the environment and human health.[67,68] H_2S is considered as the third molecule for endogenous gasotransmitters of cellular targets following nitric oxide (NO) and carbon monoxide (CO) because of its redox activity and high nucleophilic character.[69] Therefore, a negative effect on the immune response, blood pressure regulation, neurotransmission, and the endocrine, gastrointestinal, and circulatory systems has frequently occurred.[70] On the other hand, an improper balance of SO_2 can cause cancer, neurological disorders, and cardiovascular diseases. This section describes a fluorescent probe for H_2S/SO_2 dual sensing.

The design of a single fluorescent probe that responds differently to H_2S and SO_2 at the same time is usually a difficult task. In 2019, Zhang et al. reported[71] an integrated 4-azide-1,8-naphthalic anhydride and spiropyran derivative probe, **21**, where H_2S was monitored by azide reduction. Furthermore, the activated spiropyran moiety (6-NH_2-SP) acts as a new site for the recognition of SO_2 upon irradiation of UV light. The working strategy is described in Figure 20. Moreover, the probe was applied to the sensing of H_2S/SO_2 in cells and mice.

4.3. Spiropyran Derivatives as Colorimetric Probes for the Amine. Amines are being widely used for chemical and medicinal industry purposes such as biopharma, rubbers, and different chemical ingredients that have huge importance for the production of repellents, chelating agents, pesticides, soil improvers, emulsifiers, coatings, lubricants, emulsifiers, etc.[72] However, industrially used amines are reasonably toxic to humans due to their carcinogenic effects. Therefore, sensing of those toxic amines is meaningful and is an imminent task. Spiropyran (SP) is a novel photochromic material that can isomerize into two forms when exposed to visible light, allowing it to detect amines via either of its isomers.

In 2020, Xue et al.[73] employed a derivative of spiropyran **22** which contains a hydroxyl group to detect four different types of amines through a colorimetric (UV−vis) study. They were able to successfully distinguish aliphatic primary, secondary, and tertiary amines and aromatic primary, secondary, and tertiary amines through different trends and shapes with their UV−vis spectra. The primary amine recognition mechanism was proposed in Figure 21, where merocyanine typically reacts with amines to generate an indole derivative along with a Schiff base type derivative. Very similarly, aromatic primary amines were successfully recognized with probe **22** as displayed in Figure 21, in which the aromatic primary amines such as aniline or *p*-toluidine and indole derivative usually react with merocyanine to produce Schiff base type derivatives. In all cases, after amine recognition, the pink color of MC has been diminished (UV−vis) with the formation of a colorless solution.

5. FLUORESCENT pH CHEMOSENSORS

Due to its vast importance in various fields of the chemical sciences, together with industrial processes, environmental monitoring, wastewater treatment, agriculture, and physiological and pathological processes, pH monitoring has become a very active research field in recent times.[74] Various biological process which have direct relation to intracellular pH are cell metabolism, cell growth, cellular proliferation and apoptosis,[75] muscle contraction,[76] enzymatic activity,[77] homeostasis,[78] endocytosis,[79] ion transport,[80] and multidrug resistance.[81] Similarly, to maintain normalcy in metabolic processes and in subcellular activity, organelles such as lysosomes, Golgi

https://doi.org/10.1021/acsomega.2c04969
ACS Omega 2022, 7, 36988−37007

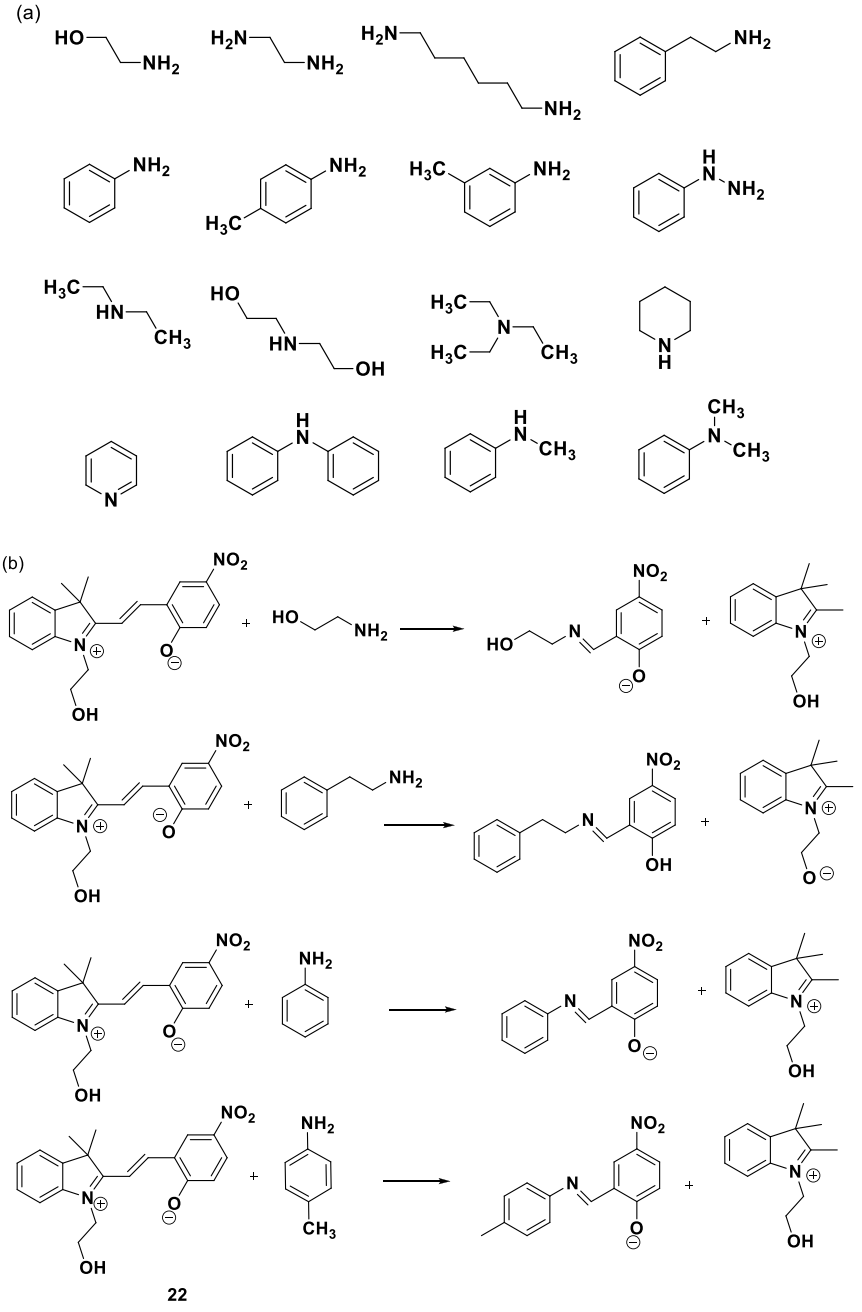

Figure 21. Proposed reactions between probe **22** and aliphatic and aromatic primary amines.

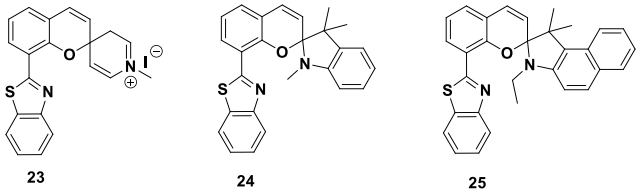

Figure 22. Structures of pH probes **23**–**25**.

apparatus, and mitochondria must maintain their individual intracellular pH levels. However, the proper and normal activities of subcellular organelles and different biological processes can be severely hampered due to abnormal or irregular pH. Abnormal pH can lead to cellular dysfunctions[82] and cause fatal diseases such as Alzheimer's disease,[83] cancer,[84] cardiopulmonary disease,[85] neurodegenerative diseases,[86] and cystic fibrosis.[87] Hence, it is necessary to monitor intracellular pH quantitatively and accurately to diagnose various diseases and to understand the physiological and pathological processes related to it.[88,89] Due to their simplicity of operation, low cost, rapid real-time response, excellent sensitivity, high selectivity, low signal-to-noise ratio, high spatiotemporal resolution, and noninvasive detection, fluorescence methods are more suitable and promising nowadays.[90−94] Spiropyrans are generally considered a class of photochromic organic dyes that switch between their closed spiropyran and open merocyanine forms under UV and visible light irradiation.[95−97] In addition to this, a change in pH can regulate reversible isomerization between the two isoforms. In acidic conditions, they switch to the open merocyanine form and return to the spiro form on increasing

https://doi.org/10.1021/acsomega.2c04969
ACS Omega 2022, 7, 36988−37007

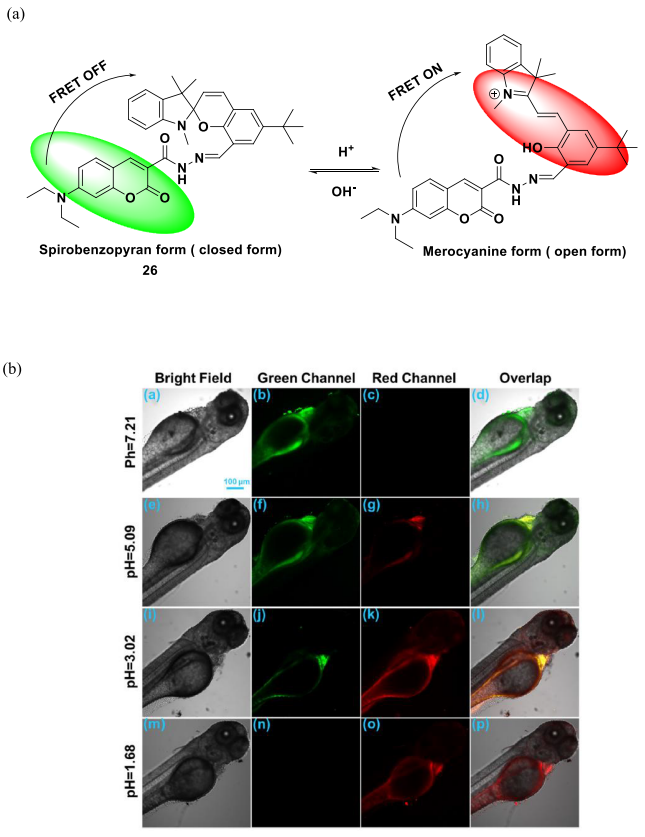

Figure 23. (a) Structure of probe **26** and its pH dependent structural changes. (b) Confocal fluorescence imaging of zebrafish treated with probe **26** (5 μM) for 20 min at pH 7.21, 5.09, 3.02, and 1.68. A 480 nm excitation wavelength was used. The images were then captured using band-pass emission filters at 500−600 and 600−700 nm, respectively, with excitation wavelengths of 488 and 515 nm. Reprinted with permission from ref 99. Copyright 2020 Elsevier.

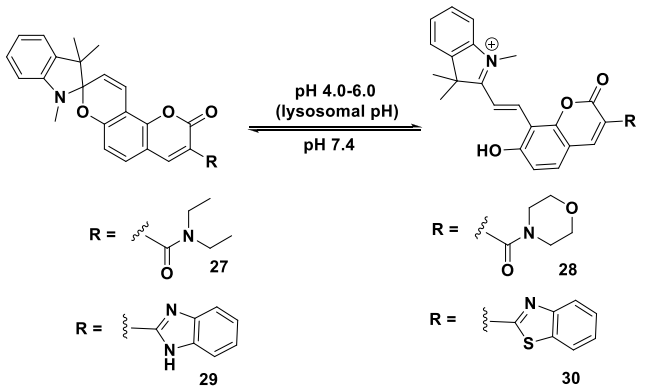

Figure 24. Structures of probes **27**−**30** and their pH dependent structural changes.

pH. As both forms exhibit different spectral properties, they provide a suitable way to design ratiometric pH probes. By taking advantage of this, researchers have reported several pH probes on the spiropyran moiety by modifying it with different functional groups.

Based on the excited-state intramolecular proton transfer (ESIPT) sensing mechanism, Zhu et al.[98] constructed three pH probes, **23**, **24**, and **25** (Figure 22), by conjugating spiropyrans with benzothiazole. All three probes were synthesized by reacting HBT (2-(2-hydroxyphenyl) benzothiazole)-CHO with three different iodide salts of pyridine and indole in the presence of piperidine in ethanol. When the pH was changed from 12.00 to 2.00, a turn-on response was exhibited by probe **23** with a fluorescence enhancement of 36-fold at 640 nm. Under similar conditions, a ratiometric response was displayed by probes **24** and **25** where the fluorescence intensity decreased at 520 and 525 nm along with an enhancement of intensity at 640 and 675 nm, respectively. This change in spectral behavior of all three probes was due to the opening of spiropyran ring in acid medium, and the open form exhibited ESIPT. The pK_a values were found to be 6.57, 4.90, and 3.95 for probes **23**, **24**, and **25**, respectively. Lastly, probe **24** was successfully used to investigate the intracellular pH change in living HeLa cells.

Using the advantages of good solubility, high fluorescence intensity, and good cell permeability of the coumarin moiety, He et al.[99] synthesized a coumarin based spiropyran pH probe, **26** (Figure 23), by a simple imine bond formation reaction between 6-(*tert*-butyl)-1′,3′,3′-trimethylspiro[chromene-2,2′-indoline]-8-carbaldehyde and 7-(diethylamino)-2-oxo-2*H*-chromene-3-carbohydrazide. The probe showed a ratiometric fluorescence change as the opened merocyanine form of the probe in acid medium exhibited a FRET-on sensing mechanism. Probe **26** displayed a 10.2-fold increase in fluorescent intensity with red shifts of 35 nm in absorption spectra and 104 nm in emission spectra on increasing acidity of the medium (pH 7.21 to 1.68). The color of the probe solution was changed from green to yellow, whereas the green fluorescence was converted to red under a similar change. With a pK_a value of 4.87, the probe exhibited good linear response within pH 4.0−6.0. Furthermore, probe **26** was applied to pH monitoring in living cells where a good ratiometric response was observed when cells were incubated with various pH media within pH 7.21−1.68 after staining with probe **26** at 37 °C for 20 min. Again, probe **26** was further used to monitor pH changes in *Pseudomonas aeruginosa* bacteria and zebrafish with promising results.

Li et al. also used different substituted coumarin moieties to construct four spiropyran based NIR pH probes, **27**, **28**, **29**, and **30** (Figure 24), to monitor pH changes in lysosomes.[100] On lowering of the pH from 6.0 to 4.0, all the probes exhibited ratiometric fluorescence changes due to in situ switching of the closed spiro form to its open form in acid medium. With pK_a values of 5.40 (**27**), 5.35 (**28**), 5.42 (**29**), and 5.26 (**30**), all the probes exhibited good lysosome specificity. Due to its best ratiometric response, probe **28** displayed a high Pearson's colocalization coefficient (PCC) value of 0.98 during colocalization study with commercial LysoTracker Green DND-26 in HepG2 cells. Further, probe **28** successfully monitored chloroquine induced lysosomal deacidification in HepG2 cells with good ratiometric response. Again, little lysosomal pH enhancement during heat strokes in living cells was also tracked ratiometrically by using probe **28**. Lastly, it was also used to monitor intracellular pH changes in HepG2 cells.

For ratiometric visualization of pH change, Zhang et al. connected near-infrared rhodol dyes with hemicyanine dye to construct pH probes **31** and **32** (Figure 25).[101] On lowering the pH from 10.2 to 3.6, acid induced a breakdown of the hemiaminal ether groups of the probes resulting in the formation of indolenium, which exhibited extended π-conjugation and was for responsible NIR emission. In absorption spectra, both probes exhibited a decline of the peak at 535 nm with gradual increases at 609 (**31**) and 622 nm (**32**). Similarly, when excited with 480 nm, the peak at 558 nm was lowered for both probes

https://doi.org/10.1021/acsomega.2c04969
ACS Omega 2022, 7, 36988−37007

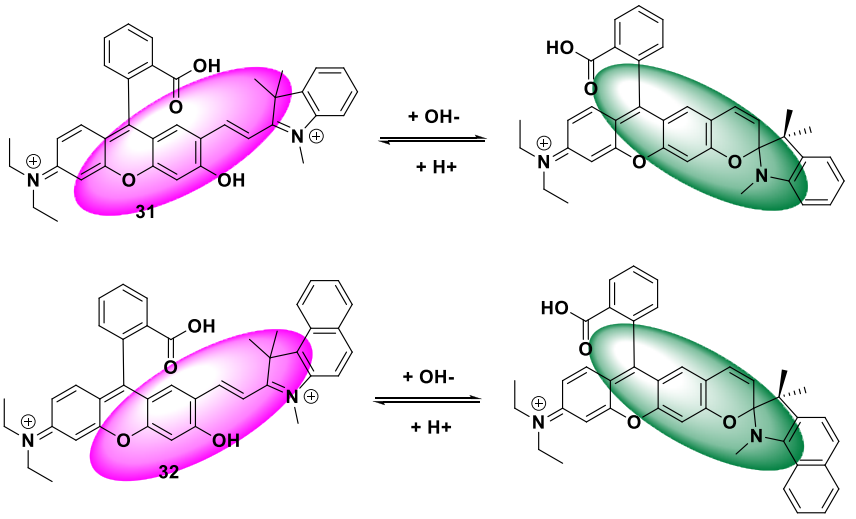

Figure 25. Structures of probes **31** and **32** and their pH dependent structural changes.

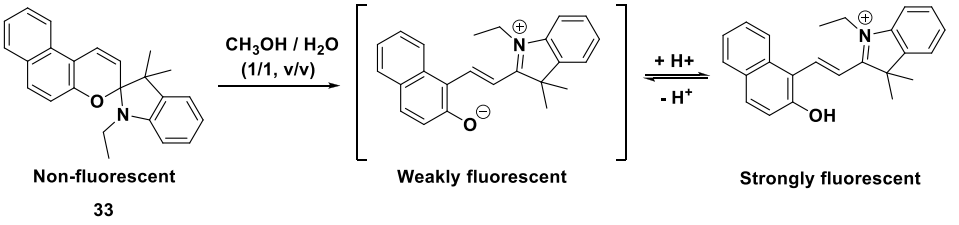

Figure 26. Structure of probe **33** and its probable sensing mechanism.

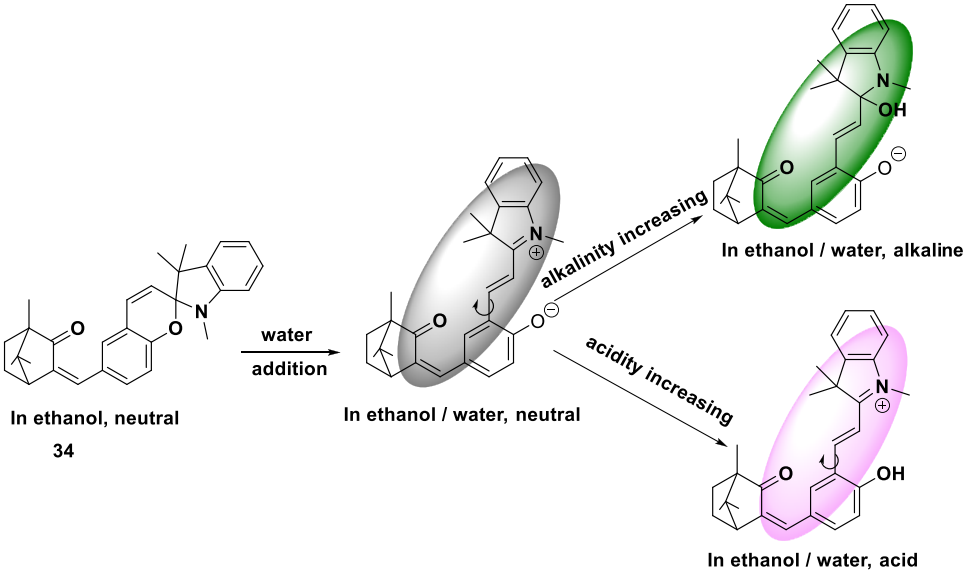

Figure 27. Structure of probe **34** and its possible sensing mechanism.

with gradual increases of the NIR peaks at 688 (**31**) and 698 nm (**32**) in emission spectra. The pK_a values were 8.26 for **31** and 7.10 for **32**. With good selectivity, the probes showed reversible responses within pH 4−10. Again, the probes were found to be mitochondria specific, and it was confirmed by a colocalization study by use of Mito Tracker blue and IR-780 cyanine dye. Using the advantage of their mitochondria targeting nature, both probes were applied to tracking nutrient starvation, rapamycin induced mitophagy, and mitochondrial acidification induced by FCCP (carbonyl cyanide 4-(trifluoromethoxy) phenylhydrazone). Moreover, the probes could successfully monitor pH changes in living HeLa cells ratiometrically. Furthermore, probe **31** was employed for in vivo imaging in *Drosophila melanogaster* first-instar larvae.

A naphthalene based spiropyran derivative, **33** (Figure 26), was synthesized through a condensation reaction between 2-hydroxy-1-naphthaldehyde and 1-ethyl-2,3,3-trimethyl-3*H*-indolium iodide salt by Xiong et al. to monitor the acidic pH

https://doi.org/10.1021/acsomega.2c04969
ACS Omega 2022, 7, 36988−37007

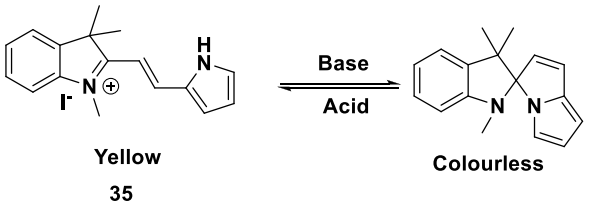

Figure 28. Structure of probe **35** and its pH dependent structural changes.

ratiometrically.[102] In CH_3OH/PBS (v/v, 1:1) medium, the spiropyran probe converted to its open form, which presented an absorption maximum at 566 nm and a weak fluorescence peak at 598 nm. But on lowering of the pH from 9.0 to 1.0, a new absorption maximum was observed at 478 nm and a strong fluorescence peak was observed at 558 nm due to protonation of the open form. This sensing mechanism was also verified by ^{1}H NMR and mass spectrometry. A clear, naked eye detectable color change was also observed, from purple to yellow. The pK_a value was calculated to be 4.85 ± 0.19. With good selectivity, photostability, and reversibility, probe **33** showed a linear response within the pH range 4.4−5.4. Importantly, the probe was successfully applied to cellular pH imaging in A549 cells.

Inspired by the good water solubility and excellent fluorescence property, Zhang et al. introduced a camphor skeleton to design a spiropyran derivative, **34** (Figure 27), to monitor both alkaline pH and viscosity.[103] Probe **34** was prepared by a condensation reaction between camphor containing a hydroxy aldehyde compound and 1,2,3,3-tetramethyl-3*H*-indolium iodide salt in the presence of a catalytic amount of piperidine in ethanol. When investigated, it was observed that in ethanol solution the closed form of probe **34** generated an absorption peak at 335 nm but addition of water in ethanol led to the formation of the open form. It displayed a new peak at 580 nm with a distinct color change from colorless to light violet. On increase of the pH (from 7.14 to 12.41), the addition reaction of the −OH group with the hemicyanine moiety of the probe led to the formation of a new absorption peak at 358 nm with a color change of the solution from light violet to pea green. A bright green fluorescence was observed at 518 nm in alkaline medium (pH 12.41) with a 105-fold fluorescent enhancement from nonfluorescent neutral medium (pH 7.14). Again, in acid medium, due to the protonation of the phenolic −OH group of the open form, the probe exhibited a new absorption peak at 452 nm with a distinct color change from light violet to yellow and a faint red fluorescence was observed. A good linear response was observed within pH 9.41−11.30, and the pK_a value was found to be 10.25. Furthermore, the probe was used in a successful analysis of the intracellular pH variation in living HeLa cells with more than 90% cell viability at a 40 μM probe concentration. It was observed that when the probe-stained HeLa cells were incubated with PBS buffer with different pHs, on increase of the pH from 7.4 to 9.5 the green fluorescence intensity gradually increased, and that proved the probe's practical applicability in intracellular pH monitoring.

The photochromic behavior of spiropyran inspired Su et al.[104] to design a spiropyrrolizine which exhibited isomerization between its spiro and merocyanine forms through baso-chromism. According to the authors, this baso-cyclization can be activated by organic and inorgainc bases when these react with the merocyanine form of probe **35** (Figure 28) to give spiropyrrolizine, and hence probe **35** can be used in alkali detection. Probe **35** was prepared by condensation between 1*H*-pyrrole-2-carbaldehyde and tetramethylindolium iodide salt in ethanol. The formation of spiropyrrolizine was also confirmed

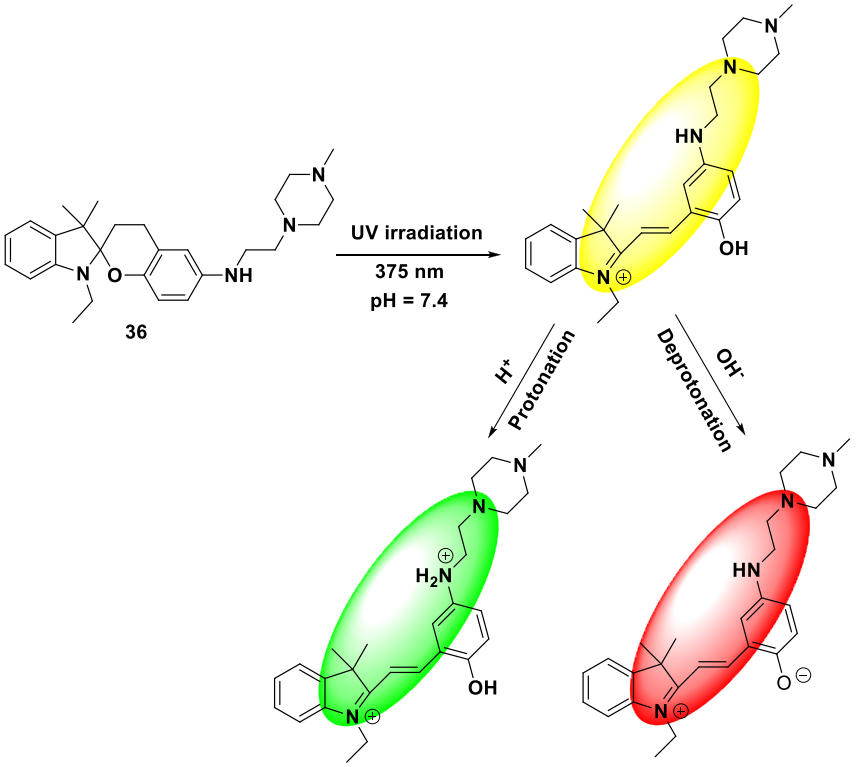

Figure 29. Structure of probe **36** and its pH dependent structural changes.

https://doi.org/10.1021/acsomega.2c04969
ACS Omega 2022, 7, 36988−37007

Table 1. Overview of Photophysical Properties of Chemosensors 1−36 for the Detection of Various Analytes and Their Applications

probe	media	sensing mechanism/probe type	excitation (nm)	emission in presence of analyte (nm)	stoichiometry	association constant	limit of detection	applications	ref
					CN^- Chemosensors				
1	CH_3CN/H_2O (1:9 v/v; pH 7.4)	−/turn on	425	583−445	1:1	$1.0 \times 10^4\ M^{-1}$	1.7 μM	test strip and imaging of live cells	25
2	THF/H_2O (4.5:5.5 v/v, 0.5 mM HEPES at pH 9)	−/colorimetric	413	−	1:1	$8.0 \times 10^4\ M^{-1}$	0.52 μM	1. quantitative analysis in cassava leaves 2. test strips	26
3, 4	ethanol/H_2O solution (9/1, v/v)	−/colorimetric	345	−	1:1	−	0.091 μM, 2.36 ppb (**3**), 0.094 μM, 2.44 ppb (**4**)	−	27
					OCl^- Chemosensor				
5	methanol−aqueous medium (1:1)	−/turn on	360	435	−	−	3 μM	−	32
					Fe^{3+}/Fe^{2+} Chemosensors				
6	DMF/H_2O (9:1, v/v)	−/turn on	378	450	1:3	−	1.93×10^{-7} M	−	36
7	THF	−	−	−	−	−	0.00298 mM	−	37
8	EtOH/H_2O (9:1)	−/turn on	360	430	3:2	−	0.77 μM	−	38
					Cu^{2+} Chemosensors				
9	acetonitrile:water (1:1, 1.0 mM HEPES, pH 7.6)	−/colorimetric	500	−	1:1	−	0.75 μM	detection of Cu^{2+} in paper strip	42
10	DMF/H_2O (9/1, v/v)	−/turn on	550	568 nm	1:1	−	14.9 fM	cell imaging	43
11	EtOH	−/colorimetric	418, 677	−	1:1	−	0.11 μM	−	44
					Hg^{2+} Chemosensor				
12	CH_3CN:water (1:1)	−	430	660	1:1	−	5.5 μM (UV−vis), 78.5 nM (fluorescence spectroscopy), and 0.62 μM (digital imaging)	digital imaging, paper strip, and real water sample	46
					Ce^{3+} Chemosensor				
13	water/ethanol (1:9 or 9:1, v/v)	−/turn on	298	380	1:1	−	1.7×10^{-6} mol/L	detection in real water sample	48
					Cr^{3+} Chemosensor				
14	methanol/H_2O (9:1, v/v)	−/colorimetric	407	−	1:1	$8.7 \times 10^3\ M^{-1}$	0.64 μM	−	50
					Ca^{2+} Chemosensor				
15	ethanol	−/turn on	375	604	1:1	$2.47 \times 10^3\ M^{-1}$	4.53×10^{-8} M	detection in paper test strips	52
					Pb^{2+} Chemosensors				
16	THF/H_2O (10/90, v/v)	FRET/ratiometric	365	480 nm↑ 635 nm↓	1:1	−	0.27 μM	1. live cell imaging 2. detection in paper test strips	54
17	MeOH/H_2O (9:1, v/v)	−/colorimetric	−	−	1:1	$1.37 \times 10^4\ M^{-1}$	0.61 μM	detection in paper test strips	55

https://doi.org/10.1021/acsomega.2c04969
ACS Omega 2022, 7, 36988−37007

Table 1. continued

probe	media	sensing mechanism/probe type	excitation (nm)	emission in presence of analyte (nm)	stoichiometry	association constant	limit of detection	applications	ref
				Li^+ Chemosensors					
18	PBS:CH_3CN (1:1, v/v)	−/turn on	550	620	−	−	4.67 μM	live cell imaging	57
				Multiple Cation Chemosensor					
19	EtOH	−/colorimetric and fluorometric	348	510 nm↑ with strong peak at 675 nm (Cu^{2+}), 510 nm↑ (Hg^{2+})	1:1 (Cu^{2+})	−	10 μM (Cu^{2+}) and 14 μM (Hg^{2+})	−	58
				PhSH Chemosensor					
20	DMSO−H_2O (PBS buffer (10.0 mM, pH 7.4))	ICT/turn off	574	620	1:2 (metal:probe)	−	0.75	real water samples test	66
				H_2S/SO_2 Chemosensor					
21	PBS/C_2H_5OH solution (v/v = 1/1, pH 7.4)	PET, CHEF/turn on	440 (for H_2S), 535 (for SO_2)	540 (for H_2S), 630 (for SO_2)		−	0.101 (for H_2S), 0.121 (for SO_2)	imaging in living cells and mice	71
				Amine Chemosensor					
22	methanol	−/colorimetric	530	−	−	−		preparation of biocompatible and bio-nontoxic nanovesicles or micelles	73
				pH Chemosensors					
23, **24**, **25**	DMSO:PBS = 1: 9, v/v	ESIPT/turn on or off, ratiometric		640 (**23**), 520−640 (**24**), 525−675 (**25**)	−	−	−	intracellular pH monitoring in living HeLa cells (**24**)	98
26	PBS buffer (1% EtOH)	FRET/ratiometric	420	525−629	−	−	−	imaging pH change in living cells, bacteria, and zebrafish	99
27, **28**, **29**, **30**	phosphate buffer solution	−/ratiometric	375 (**27**, **28**), 405 (**29**, **30**)	460−662 (**28**), −/660 (**27**), −/692 (**29**), −/693 (**30**)		−		monitoring intracellular pH change, chloroquine, and heat shock induced pH change	100
31, **32**	buffers containing 30% ethanol	−/ratiometric	480	558−688 (**31**), 558−698 (**32**)	−	−	−	intracellular pH change, in vivo imaging of pH in *D. melanogaster* first-instar larvae, FCCP induced mitochondrial acidification, nutrient starvation, and rapamycin induced mitophagy	101
33	CH_3OH/PBS (v/v, 1:1)	−/ratiometric	566 and 478	598−558	−	−	−	cellular pH imaging in A549 cells	102
34	ethanol/water (v/v = 4/6)	ICT/turn on or off	420	518	−	−	−	intracellular pH monitoring in living HeLa cells	103
35	acetonitrile and DMSO solution	−/turn on or off	−	520	−	−	−	−	104
36	PBS buffer solutions	ICT/ratiometric	487	595−563, 595−664		−		intracellular pH change induced by UV light during programmed cell death	105

https://doi.org/10.1021/acsomega.2c04969
ACS Omega 2022, 7, 36988−37007

by ^{1}H NMR and DFT studies. On increasing the concentration of triethylamine (from 0 to 50 equiv) in acetonitrile and DMSO solution of the probe at a concentration of 25 μM, the probe exhibited a gradual increase of the absorption peak at 291 nm with a rapid decrease of the peak at 462 nm. As a result, the yellow open merocyanine form converted to the colorless closed spiro form. In emission spectra the peak at 520 nm also showed a gradual decrease in acetonitrile solvent in a similar change to form the nonfluorescent spiro form. Again, the probe was found to be reversible when examined with triethylamine and TFA (trifluoroacetic acid).

Jiang et al. designed a light-activated "cycle reversible ICT" based spiropyran pH probe, **36** (Figure 29).[105] During the design of probe **36** the authors introduced *N*-methylpiperazine as terminal group to reduce toxicity and the flexible ethylcarbon chain to control the water/oil amphipathy. More importantly, hydroxyl group and imide group of the probe regulated cyclic invertibility due to their synergistic protonation−deprotonation process. The probe revealed a turn-on fluorescence response with yellow emission at 595 nm on UV light irradiation as its nonfluorescent spiropyran form converted to a fluorescent hemicyanine form. Then, on change of the pH from 7.53 to 8.46, the phenolic −OH group of the open form of the probe deprotonated in the basic medium and, as a result, the probe produced a new emission peak at 664 nm with red fluorescence. Again, with increasing acidity (pH from 7.32 to 3.87), a new emission peak at 563 nm with green fluorescence was observed and the yellow emission peak at 595 nm gradually lowered in both acid and basic media. Moreover, with the use of the probe a trace change of intracellular pH was monitored during programmed cell death caused by UV light irradiation. During the experiment, in HepG2 cells it was observed that, upon exposure to UV light for 120 min, the fluorescence intensity of the yellow channel lowered and a stable red channel intensity gradually increased, which was the indication of cell apoptosis where cells gradually become alkaline under programmed death.

Table 1 summarizes the photophysical properties of the chemosensors (**1**−**36**) discussed in this review.

6. CONCLUSION AND PERSPECTIVES

In this review, we highlighted the design strategy and widespread use of spiropyran derivatives in the detection of various metal ions, anions, neutral analytes, and pH. The interswitching ability between SP and MC isoforms which exhibit different spectral properties as well as protonation−deprotonation of the MC form allows the researcher to use it suitably in sensing purposes by developing different colorimetric and fluorometric probes. Along with this, different modifications can be made in the SP form to selectively recognize any target of interest, and that reveals its versatility in the recognition field. Not only that, a small change in the functional group of spiropyran can make it more sensitive toward certain analytes. Due to the novelty of spiropyran, it attracts the attention of researchers to make it a more unique detection tool with innovative applications. In spite of the different advantages, there are some major drawbacks: (1) The syntheses of spiropyran derivatives and their purification are difficult.[100] (2) Due to the nonfluorescent nature of the SP form, ratiometric fluorescent probes on spiropyran derivatives are lacking.[101] (3) The practical application of rapid detection of analytes is also hampered as SP derivatives are sparingly water-soluble and its ring opening needs photoinduction.[26]

Moreover, the following properties should be prioritized for more precise sensing by using this platform: (1) NIR design is required because it provides deep tissue penetration strength with minimal photo damage to the sample. (2) The probe should be ratiometric in order to eliminate environmental factors, probe concentration fluctuations, and instrumental errors. (3) Probes having a large Stokes shift can reduce excitation interference and autofluorescence of biosamples, so it should be considered during probe design. (4) Some of the reported probes have no practical applications. Therefore, probes with more innovative practical applications should be explored. (5) Because probes with AIE and FRET sensing mechanisms are still in the early stages, they should be investigated further in the near future. (6) Biocompatible probes with good water solubility, cell permeability, and photostability with low cytotoxicity should be used for biological applications. (7) Some of the probes suffer from interference from other analytes, and that should be resolved with more selective probes.

AUTHOR INFORMATION

Corresponding Author

Ajit Kumar Mahapatra − *Department of Chemistry, Indian Institute of Engineering Science and Technology, Shibpur, Howrah 711103 West Bengal, India;* orcid.org/0000-0003-4369-7197; Email: akmahapatra@chem.iiests.ac.in

Authors

Moumi Mandal − *Department of Chemistry, Indian Institute of Engineering Science and Technology, Shibpur, Howrah 711103 West Bengal, India*

Dipanjan Banik − *Department of Chemistry, Indian Institute of Engineering Science and Technology, Shibpur, Howrah 711103 West Bengal, India*

Anirban Karak − *Department of Chemistry, Indian Institute of Engineering Science and Technology, Shibpur, Howrah 711103 West Bengal, India*

Saikat Kumar Manna − *Department of Chemistry, Haldia Government College, Debhog, Haldia, Purba Medinipur 721657 West Bengal, India*

Complete contact information is available at: https://pubs.acs.org/10.1021/acsomega.2c04969

Notes

The authors declare no competing financial interest.

ACKNOWLEDGMENTS

D.B. is grateful to the CSIR, New Delhi, India [File No. 08/003(0143)/2020-EMR-I], for providing a fellowship. A.K. thanks IIEST, Shibpur, for sponsoring an institute fellowship.

REFERENCES

(1) Such, G.; Evans, R. A.; Yee, L. H.; Davis, T. J. Factors influencing photochromism of spiro-compounds within polymeric matrices. *Macromol. Sci. Part C* **2003**, *43*, 547−579.

(2) Chibisov, A. K.; Görner, H. Photochromism of spirobenzopyranindolines and spironaphthopyranindolines. *Phys. Chem. Chem. Phys.* **2001**, *3*, 424−431.

(3) Gehrtz, M.; Bräuchle, C.; Voitländer. Photochromic forms of 6-nitrobenzospiropyran. Emission spectroscopic and ODMR investigations. *J. Am. Chem. Soc.* **1982**, *104*, 2094−2101.

(4) Weis, L. D.; Evans, T. R.; Leermakers, P. A. Electronic spectra and photochemistry of adsorbed organic molecules. VI. Binding effects of silica as a mechanistic probe in systems of photochemical interest. *J. Am. Chem. Soc.* **1968**, *90*, 6109−6118.

(5) Bandara, H. M. D.; Burdette, S. C. Photoisomerization in different classes of azobenzene. *Chem. Soc. Rev.* **2012**, *41*, 1809−1825.
(6) Fischer, E.; Hirshberg, Y. Formation of coloured forms of spirans by low-temperature irradiation. *J. Chem. Soc.* **1952**, 4522−4524.
(7) Lukyanov, B. S.; Lukyanova, M. B. *Chem. Heterocycl. Compd.* **2005**, *41*, 281−311.
(8) Minkin, V. I. Spiropyrans: synthesis, properties, and application. *Chem. Rev.* **2004**, *104*, 2751−2776.
(9) Menju, A.; Hayashi, K.; Irie, M. Photoresponsive polymers. 3. Reversible solution viscosity change of poly (methacrylic acid) having spirobenzopyran pendant groups in methanol. *Macromolecules* **1981**, *14*, 755−758.
(10) Helmy, S.; Leibfarth, F. A.; Oh, S.; Poelma, J. E.; Hawker, C. J.; Read de Alaniz, J. Photoswitching using visible light: a new class of organic photochromic molecules. *J. Am. Chem. Soc.* **2014**, *136*, 8169−8172.
(11) Davis, A. D.; Hamilton, A.; Yang, J.; Cremar, L. D.; Van Gough, D.; Potisek, S. L.; Ong, M. T.; Braun, P. V.; Martınez, T. J.; White, S. R.; Moore, J. S.; Sottos, N. R. *Nature* **2009**, *459*, 68−72.
(12) O'Bryan, G.; Wong, B. M.; McElhanon, J. R. *ACS Appl. Mater. Interfaces* **2010**, *2*, 1594−1600.
(13) Wong, B. M.; Ye, S. H.; O'Bryan, G. *Nanoscale* **2012**, *4*, 1321−1327.
(14) Brügner, O.; Reichenbach, T.; Sommer, M.; Walter, M. *J. Phys. Chem. A* **2017**, *121*, 2683−2687.
(15) Swansburg, S.; Buncel, E.; Lemieux, R. P. Thermal racemization of substituted indolinobenzospiropyrans: Evidence of competing polar and nonpolar mechanisms. *J. Am. Chem. Soc.* **2000**, *122*, 6594−6600.
(16) Wojtyk, J. T. C.; Wasey, A.; Kazmaier, P. M.; Hoz, S.; Buncel, E. Thermal Reversion Mechanism of N-Functionalized Merocyanines to Spiropyrans: A Solvatochromic, Solvatokinetic, and Semiempirical Study. *J. Phys. Chem. A* **2000**, *104*, 9046−9055.
(17) Satoh, T.; Sumaru, K.; Takagi, T.; Takai, K.; Kanamori, T. Isomerization of spirobenzopyrans bearing electron-donating and electron-withdrawing groups in acidic aqueous solutions. *Phys. Chem. Chem. Phys.* **2011**, *13*, 7322−7329.
(18) Ali, A. A.; Kharbash, R.; Kim, Y. Chemo- and biosensing applications of spiropyran and its derivatives -A review. *Anal. Chim. Acta* **2020**, *1110*, 199−223.
(19) Kortekaas, L.; Browne, W. R. The evolution of spiropyran: fundamentals and progress of an extraordinarily versatile photochrome. *Chem. Soc. Rev.* **2019**, *48*, 3406−3424.
(20) Dey, N.; Bhattacharya, S. Switchable optical probes for simultaneous targeting of multiple anions. *Chem. - Asian J.* **2020**, *15*, 1759−1779.
(21) Li, Q.; Shao, S.-J. Progress on optical probes for hydrogen sulfate anion sensing. *Chin. J. Anal. Chem.* **2017**, *45*, 1248−1256.
(22) Awual, M. R.; Hasan, M. M.; Khaleque, M. A.; Sheikh, M. C. Treatment of copper (II) containing wastewater by a newly developed ligand based facial conjugate materials. *Chem. Eng. J.* **2016**, *288*, 368−376.
(23) Yang, Y.; Zhao, Q.; Feng, W.; Li, F. Luminescent Chemodosimeters for Bioimaging. *Chem. Rev.* **2013**, *113*, 192−270.
(24) Kulig, K. W. *Cyanide Toxicity*; U.S. Department of Health and Human Services: Atlanta, GA, 1991.
(25) Mahapatra, A. K.; Maiti, K.; Manna, S. K.; Maji, R.; Mukhopadhyay, C. D.; Pakhira, B.; Sarkar, S. Unique fluorogenic ratiometric fuorescent chemodosimeter for rapid sensing of CN^- in Water. *Chem. - Asian J.* **2014**, *9*, 3623−3632.
(26) Pattaweepaiboon, S.; Kongmon, W.; Thaweechai, T.; Kaewchangwat, N.; Thanayupong, E.; Suttisintong, K.; Sirisaksoontorn, W. A spiropyran-based colorimetric probe for quantitative analysis of cyanide ions in cassava leaves. *Dyes Pigm.* **2020**, *173*, 108005.
(27) Sanjabi, S.; Keyvan Rad, J.; Mahdavian, R. A. Spiropyran and spironaphthoxazine based opto-chemical probes for instant ion detection with high selectivity and sensitivity to trace amounts of cyanide. *J. Photochem. Photobiol. A: Chem.* **2022**, *424*, 113626.
(28) Chen, X.; Tian, X.; Shin, I.; Yoon, J. Fluorescent and luminescent probes for detection of reactive oxygen and nitrogen species. *Chem. Soc. Rev.* **2011**, *40*, 4783−4804.
(29) Marcinkiewicz, J.; Chain, B.; Nowak, B.; Grabowska, A.; Bryniarski, K.; Baran, J. Antimicrobial and cytotoxic activity of hypochlorous acid: interactions with taurine and nitrite. *Inflamm. Res.* **2000**, *49*, 280−289.
(30) Rudolph, V.; Andrie, R. P.; Rudolph, T. K.; Friedrichs, K.; Klinke, A.; HirschHoffmann, B.; Schwoerer, A. P.; Lau, D.; Fu, X.; Klingel, K.; Sydow, K.; Didie, M.; Seniuk, A.; von Leitner, E.-C.; Szoecs, K.; Schrickel, J. W.; Treede, H.; Wenzel, U.; Lewalter, T.; Nickenig, G.; Zimmermann, W.-H.; Meinertz, T.; Boger, R. H.; Reichenspurner, H.; Freeman, B. A.; Eschenhagen, T.; Ehmke, H.; Hazen, S. L.; Willems, S.; Baldus, S. Myeloperoxidase acts as a profibrotic mediator of atrial fibrillation. *Nat. Med.* **2010**, *16*, 470−474.
(31) Whiteman, M.; Rose, P.; Siau, J. L.; Cheung, N. S.; Tan, G. S.; Halliwell, B.; Armstrong, J. S. Hypochlorous acid-mediated mitochondrial dysfunction and apoptosis in human hepatoma HepG2 and human fetal liver cells: role of mitochondrial permeability transition. *Free Radic. Biol. Med.* **2005**, *38*, 1571−1584.
(32) Samanta, S.; Halder, S.; Manna, U.; Das, G. Specific detection of hypochlorite: a cyanine-based turn-on fluorescent sensor. *J. Chem. Sci.* **2019**, *131*, 36.
(33) Yeung, M. C. L.; Yam, V. W. W. Luminescent cation sensors: from host−guest chemistry, supramolecular chemistry to reaction-based mechanisms. *Chem. Soc. Rev.* **2015**, *44*, 4192−4202.
(34) Chua, M. H.; Zhou, H.; Zhu, Q.; Tang, B. Z.; Xu, J. W. Recent advances in cation sensing using aggregation-induced emission. *Mater. Chem. Front.* **2021**, *5*, 659−708.
(35) Rattanopas, S.; Piyanuch, P.; Wisansin, K.; Charoenpanich, A.; Sirirak, J.; Phutdhawong, W.; Wanichacheva, N. Indole-based fluorescent sensors for selective sensing of Fe2+ and Fe3+ in aqueous buffer systems and their applications in living cells. *J. Photochem. Photobiol. A: Chem.* **2019**, *377*, 138−148.
(36) Zhang, R.; Hu, L.; Xu, Z.; Song, Y.; Li, H.; Zhang, X.; Gao, X.; Wang, M.; Xian, C. A highly selective probe for fluorescence turn-on detection of Fe3+ ion based on a novel spiropyran derivative. *J. Mol. Struct.* **2020**, *1204*, 127481.
(37) Yang, Z.; Wang, F.; Liu, H. Dual responsive spiropyran-ended poly (N-vinyl caprolactam) for reversible complexation with metal ions. *J. Polym. Res.* **2019**, *26*, 89.
(38) Zhang, D.; Qi, Y.; Li, Y.; Song, Y.; Xian, C.; Li, H.; Cong, P. A New Spiropyran-Based Fluorescent Probe for Dual Sensing of Ferrous Ion and pH. *J. Fluoresc.* **2021**, *31*, 1133−1141.
(39) Yun, S. H.; Xia, L.; Edison, T. N. J. I.; Pandurangan, M.; Kim, D. H.; Kim, S. H.; Lee, Y. R. Highly selective fluorescence turn-on sensor for Cu^{2+} ions and its application in confocal imaging of living cells. *Sens. Actuators B Chem.* **2017**, *240*, 988−995.
(40) Sabari, P.; Ravikanth, M. 3-Pyrrolyl BODIPY Based Selective Cu2+ Ion "Off-On" Fluorescent Sensor. *J. Chem. Sci.* **2021**, *133*, 59.
(41) Mahapatra, A. K.; Karak, A.; Manna, S. K. Triphenylamine-based small-molecule fluorescent probes. *Anal. Methods* **2022**, *14*, 972.
(42) Kumar, A.; Kumar, S. A benzothiazolinic spiropyran for highly selective, sensitive and visible light-controlled detection of copper ions in aqueous solution. *J. Photochem. Photobiol. A: Chem.* **2020**, *390*, 112265.
(43) Xuan, J.; Tian, J. Heating promoted fluorescent recognition of Cu^{2+} with high selectivity and sensitivity based on spiropyran derivative. *Anal. Chim. Acta* **2019**, *1061*, 161−168.
(44) Trevino, K. M.; Tautges, B. K.; Kapre, R.; Franco, F. C., Jr; Or, V. W.; Balmond, E. I.; Shaw, J. T.; Garcia, J.; Louie, A. Y. Highly sensitive and selective spiropyran-based sensor for Copper (II) quantification. *ACS omega.* **2021**, *6*, 10776−10789.
(45) Mei, Q.; Wang, L.; Tian, B.; Yan, F.; Zhang, B.; Huang, W.; Tong, B. A highly selective and naked-eye sensor for Hg^{2+} based on quinazoline-4 (3H)-thione. *New J. Chem.* **2012**, *36*, 1879−1883.
(46) Kumar, A.; Sahoo, P. R.; Arora, P.; Kumar, S. A light controlled, sensitive, selective and portable spiropyran based receptor for mercury

https://doi.org/10.1021/acsomega.2c04969
ACS Omega 2022, 7, 36988−37007

ions in aqueous solution. *J. Photochem. Photobiol. A: Chem.* **2019**, *384*, 112061.
(47) Zheng, X. L.; Liu, Y.; Pan, M.; Lü, X. Q.; Zhang, J. Y.; Zhao, C. Y.; Tong, Y. X.; Su, C. Y. Bright blue-emitting Ce^{3+} complexes with encapsulating polybenzimidazole tripodal ligands as potential electroluminescent devices. *Angew. Chem., Int. Ed.* **2007**, *46*, 7399−7403.
(48) Luo, X.; Chen, D.; Xu, Z.; Song, Y.; Li, H.; Xian, C. A fluorescent probe based on a spiropyran for sensitive detection of Ce^{3+} ion. *J. Rare Earths.* **2020**, *38*, 445−450.
(49) Jiang, T.; Bian, W.; Kan, J.; Sun, Y.; Ding, N.; Li, W.; Zhou, J. Sensitive and rapid detection of Cr^{3+} in live cells by a red turn-on fluorescent probe. *Spectrochim. Acta, Part A* **2021**, *245*, 118903.
(50) Liu, G.; Cui, C.; Jiang, L.; Gao, H.; Gao, J. Visible light-induced hydrogels towards reversible adsorption and desorption based on trivalent chromium in aqueous solution. *React. Funct. Polym.* **2021**, *163*, 104886.
(51) Yao, K.; Chang, Y.; Li, B.; Yang, H.; Xu, K. A novel coumarin-based fluorescent sensor for Ca^{2+} and sequential detection of F^- and its live cell imaging. *Spectrochim. Acta, Part A* **2019**, *216*, 385−394.
(52) Wang, L.; Yao, Y.; Wang, J.; Dong, C.; Han, H. Selective sensing Ca^{2+} with a spiropyran-based fluorometric probe. *Luminescence.* **2019**, *34*, 707−714.
(53) Meng, X.; Cao, D.; Hu, Z.; Han, X.; Li, Z.; Ma, W. A highly sensitive and selective chemosensor for Pb^{2+} based on quinoline−coumarin. *RSC Adv.* **2018**, *8*, 33947−33951.
(54) Ho, F.-C.; Huang, K.-H.; Cheng, H.-W.; Huang, Y.-J.; Nhien, P. Q.; Wu, C.-H.; Wu, J. I.; Chen, S.-Y.; Lin, H.-C. FRET processes of bi-fluorophoric sensor material containing tetraphenylethylene donor and optical-switchable merocyanine acceptor for lead ion (Pb^{2+}) detection in semi-aqueous media. *Dyes Pigm.* **2021**, *189*, 109238.
(55) Liu, G.; Li, Y.; Cui, C.; Wang, M.; Gao, H.; Gao, J.; Wang, J. Solvatochromic spiropyran-a facile method for visualized, sensitive and selective response of lead (Pb^{2+}) ions in aqueous solution. *J. Photochem. Photobiol. A: Chem.* **2022**, *424*, 113658.
(56) Kamenica, M.; Kothur, R. R.; Willows, A.; Patel, B. A.; Cragg, P. J. Lithium ion sensors. *Sensors.* **2017**, *17*, 2430.
(57) Kang, J.; Li, E.; Cui, L.; Shao, Q.; Yin, C.; Cheng, F. Lithium ion specific fluorescent reversible extraction-release based on spiropyran isomerization combining crown ether coordination and its bioimaging. *Sens. Actuators B Chem.* **2021**, *327*, 128941.
(58) Wang, Y.; Xu, Z.; Dai, X.; Li, H.; Yu, S.; Meng, W. A new spiropyran-based sensor for colorimetric and fluorescent detection of divalent Cu^{2+} and Hg^{2+} ions and trivalent Ce^{3+}, Cr^{3+} and Al^{3+} ions. *J. Fluoresc.* **2019**, *29*, 569−575.
(59) Wu, L.; Huang, C.; Emery, B. P.; Sedgwick, A. C.; Bull, S. D.; He, X.-P.; Tian, H.; Yoon, J.; Sessler, J. L.; James, T. D. Förster resonance energy transfer (FRET)-based small-molecule sensors and imaging agents. *Chem. Soc. Rev.* **2020**, *49*, 5110−5139.
(60) Amrolia, P.; Sullivan, S. G.; Stern, A.; Munday, R. Toxicity of aromatic thiols in the human red blood cell. *J. Appl. Toxicol.* **1989**, *9*, 113−118.
(61) Love, J. C.; Estroff, L. A.; Kriebel, J. K.; Nuzzo, R. G.; Whitesides, G. M. Self-assembled monolayers of thiolates on metals as a form of nanotechnology. *Chem. Rev.* **2005**, *105*, 1103−1170.
(62) Hathaway, G. J.; Proctor, N. H. *Proctor and Hughes' Chemical Hazards of the Workplace*; John Wiley & Sons: 2004; pp 575−576.
(63) Munday, R.; Manns, E. Toxicity of aromatic disulphides. III. In vivo haemolytic activity of aromatic disulphides. *J. Appl. Toxicol.* **1985**, *5*, 414−417.
(64) Juneja, T. R.; Gupta, R. L.; Samanta, S. Activation of monocrotaline, fulvine and their derivatives to toxic pyrroles by some thiols. *Toxicol. Lett.* **1984**, *21*, 185−189.
(65) Jiang, W.; Fu, Q. Q.; Fan, H. Y.; Ho, J.; Wang, W. A highly selective fluorescent probe for thiophenols. *Angew. Chem., Int. Ed.* **2007**, *46*, 8445−8448.
(66) Yang, L.; Li, Y.; Song, H.; Zhang, H.; Yang, N.; Peng, Q.; Ji, L.; He, G. *Dyes Pigm.* **2020**, *175*, 108154.
(67) Jiao, X. Y.; Li, Y.; Niu, J. Y.; Xie, X. L.; Wang, X.; Tang, B. Small-molecule fluorescent probes for imaging and detection of reactive oxygen, nitrogen, and sulfur species in biological systems. *Anal. Chem.* **2018**, *90*, 533−555.
(68) Liu, C. R.; Chen, N. W.; Shi, W.; Peng, B.; Zhao, Y.; Ma, H. M.; Xian, M. Rational design and bioimaging applications of highly selective fluorescence probes for hydrogen polysulfides. *J. Am. Chem. Soc.* **2014**, *136*, 7257−7260.
(69) Li, J. L.; Meng, Z. Q. The role of sulfur dioxide as an endogenous gaseous vasoactive factor in synergy with nitric oxide. *Nitric Oxide* **2009**, *20*, 166−174.
(70) Guo, W.; Cheng, Z.-Y.; Zhu, Y.-Z. Hydrogen sulfide and translational medicine. *Acta Pharmacol. Sin.* **2013**, *34*, 1284−1291.
(71) Zhang, W.; Huo, F.; Yin, C. Photocontrolled single-/dual-site alternative fluorescence probes distinguishing detection of H_2S/SO_2 *in vivo*. *Org. Lett.* **2019**, *21*, 5277−5280.
(72) Zhang, S. G. *Handbook on Practical Fine Chemicals*; Chemical Industry Press: Beijing, 1996.
(73) Xue, Y.; Tian, J.; Tian, W.; Zhang, K.; Xuan, J.; Zhang, X. *Spectrochim. Acta, Part A* **2021**, *250*, 119385.
(74) Ma, J.; Li, W.; Li, J.; Shi, R.; Yin, G.; Wang, R. A Small Molecular pH-Dependent Fluorescent Probe for Cancer Cell Imaging in Living Cell. *Talanta* **2018**, *182*, 464−469.
(75) Lagadic-Gossmann, D.; Huc, L.; Lecureur, V. Alterations of Intracellular pH Homeostasis in Apoptosis: Origins and Roles. *Cell Death Differ.* **2004**, *11*, 953−961.
(76) Nogueira, L.; Shiah, A. A.; Gandra, P. G.; Hogan, M. C. Ca^{2+}-Pumping Impairment during Repetitive Fatiguing Contractions in Single Myofibers: Role of Cross-Bridge Cycling. *Am. J. Physiol. Regul. Integr. Comp. Physiol.* **2013**, *305*, R118−R125.
(77) Barott, K. L.; Barron, M. E.; Tresguerres, M. Identification of a Molecular pH Sensor in Coral. *Proc. R Soc. B* **2017**, *284*, 20171769.
(78) Yao, H.; Haddad, G. G. Calcium and pH Homeostasis in Neurons during Hypoxia and Ischemia. *Cell Calcium.* **2004**, *36*, 247−255.
(79) Shen, Y.; Rosendale, M.; Campbell, R. E.; Perrais, D. pHuji, a pH-Sensitive Red Fluorescent Protein for Imaging of Exo- and Endocytosis. *J. Cell Biol.* **2014**, *207*, 419−432.
(80) Ramirez, P.; Mafe, S.; Alcaraz, A.; Cervera, J. Modeling of pH Switchable Ion Transport and Selectivity in Nanopore Membranes with Fixed Charges. *J. Phys. Chem. B* **2003**, *107*, 13178−13187.
(81) Simon, S.; Roy, D.; Schindler, M. Intracellular pH and the Control of Multidrug Resistance. *Proc. Natl. Acad. Sci. U.S.A.* **1994**, *91*, 1128−1132.
(82) Hou, J. T.; Ren, W. X.; Li, K.; Seo, J.; Sharma, A.; Yu, X. Q.; Kim, J. S. Fluorescent Bioimaging of pH: From Design to Applications. *Chem. Soc. Rev.* **2017**, *46*, 2076−2090.
(83) Fang, B.; Wang, D.; Huang, M.; Yu, G.; Li, H. Hypothesis on the Relationship between the Change in Intracellular PH and Incidence of Sporadic Alzheimer's Disease or Vascular Dementia. *Int. J. Neurosci.* **2010**, *120*, 591−595.
(84) Swietach, P.; Wigfield, S.; Cobden, P.; Supuran, C. T.; Harris, A. L.; Vaughan-Jones, R. D. Tumor-Associated Carbonic Anhydrase 9 Spatially Coordinates Intracellular PH in Three- Dimensional Multicellular Growths. *J. Biol. Chem.* **2008**, *283*, 20473−20483.
(85) He, X.; Xu, W.; Xu, C.; Ding, F.; Chen, H.; Shen, J. Reversible Spiropyran-Based Chemosensor with pH-Switches and Application for Bioimaging in Living Cells Pseudomonas aeruginosa and Zebrafish. *Dyes Pigm.* **2020**, *180*, 108497.
(86) Wang, C.; Telpoukhovskaia, M. A.; Bahr, B.; Chen, X.; Gan, L. Endo-Lysosomal Dysfunction: A Converging Mechanism in Neurodegenerative Diseases. *Curr. Opin. Neurobiol.* **2018**, *48*, 52−58.
(87) Chen, J. H.; Xu, W.; Sheppard, D. N. Altering Intracellular pH Reveals the Kinetic Basis of Intraburst Gating in the CFTR Cl-Channel. *J. Physiol.* **2017**, *595*, 1059−1076.
(88) Deutsch, C.; Taylor, J. S.; Wilson, D. F. Regulation of Intracellular pH by Human Peripheral Blood Lymphocytes as Measured by 19F NMR. *Proc. Natl. Acad. Sci. U.S.A.* **1982**, *79*, 7944−7948.

https://doi.org/10.1021/acsomega.2c04969
ACS Omega 2022, 7, 36988−37007

(89) Anemone, A.; Consolino, L.; Arena, F.; Capozza, M.; Longo, D. L. Imaging Tumor Acidosis: A Survey of the Available Techniques for Mapping in Vivo Tumor pH. *Cancer Metastasis Rev.* **2019**, *38*, 25−49.
(90) Banik, D.; Manna, S. K.; Mahapatra, A. K. Recent Development of Chromogenic and Fluorogenic Chemosensors for the Detection of Arsenic Species: Environmental and Biological Applications. *Spectrochim. Acta, Part A* **2021**, *246*, 119047.
(91) Banik, D.; Manna, S. K.; Maiti, A.; Mahapatra, A. K. Recent Advancements in Colorimetric and Fluorescent pH Chemosensors: From Design Principles to Applications. *Crit. Rev. Anal. Chem.* **2022**, DOI: 10.1080/10408347.2021.2023002.
(92) Yang, Y. M.; Zhao, Q.; Feng, W.; Li, F. Y. Luminescent Chemodosimeters for Bioimaging. *Chem. Rev.* **2013**, *113*, 192−270.
(93) Yin, J.; Huang, L.; Wu, L.; Li, J.; James, T. D.; Lin, W. Small Molecule Based Fluorescent Chemosensors for Imaging the Microenvironment within Specific Cellular Regions. *Chem. Soc. Rev.* **2021**, *50*, 12098−12150.
(94) Han, H.-H.; Tian, H., Jr.; Zang, Y.; Sedgwick, A. C.; Li, J.; Sessler, J. L.; He, X.-P.; James, T. D. Small-Molecule Fluorescence-Based Probes for Interrogating Major Organ Diseases. *Chem. Soc. Rev.* **2021**, *50*, 9391−9429.
(95) Klajn, R. Spiropyran-Based Dynamic Materials. *Chem. Soc. Rev.* **2014**, *43*, 148−184.
(96) Seefeldt, B.; Kasper, R.; Beining, M.; Mattay, J.; Arden-Jacob, J.; Kemnitzer, N.; Drexhage, K. H.; Heilemann, M.; Sauer, M. Spiropyrans as Molecular Optical Switches. *Photochem. Photobiol. Sci.* **2010**, *9*, 213−220.
(97) Xie, X.; Mistlberger, G.; Bakker, E. Reversible Photodynamic Chloride-Selective Sensor Based on Photochromic Spiropyran. *J. Am. Chem. Soc.* **2012**, *134*, 16929−16932.
(98) Zhu, J.; Gao, Q.; Tong, Q.; Wu, G. Fluorescent probes based on benzothiazole-spiropyran derivatives for pH monitoring in vitro and in vivo. *Spectrochim. Acta, Part A* **2020**, *225*, 117506.
(99) He, X.; Xu, W.; Xu, C.; Ding, F.; Chen, H.; Shen, J. Reversible spiropyran-based chemosensor with pH-switches and application for bioimaging in living cells, *Pseudomonas aeruginosa* and zebrafish. *Dyes Pigm.* **2020**, *180*, 108497.
(100) Li, J.; Li, X.; Jia, J.; Chen, X.; Lv, Y.; Guo, Y.; Li, J. A ratiometric near-infrared fluorescence strategy based on spiropyran *in situ* switching for tracking dynamic changes of live-cell lysosomal pH. *Dyes Pigm.* **2019**, *166*, 433−442.
(101) Zhang, Y.; Xia, S.; Mikesell, L.; Whisman, N.; Fang, M.; Steenwinkel, T.; Chen, K.; Luck, R. L.; Werner, T.; Liu, H. Near-Infrared Hybrid Rhodol Dyes with Spiropyran Switches for Sensitive Ratiometric Sensing of pH Changes in Mitochondria and *Drosophila melanogaster* First-Instar Larvae. *ACS Appl. Bio Mater.* **2019**, *2*, 4986−4997.
(102) Xiong, K.; Yin, C.; Yue, Y.; Huo, F. A near-infrared ratiometric fluorescence probe base on spiropyran derivative for pH and its application in living cells. *Spectrochim. Acta, Part A* **2019**, *223*, 117350.
(103) Zhang, Y.; Qin, A.; Gong, S.; Li, M.; Meng, Z.; Liang, Y.; Shen, Z.; Wang, Z.; Wang, S. Two birds with one stone: A novel dual-functional fluorescent probe for simultaneous monitoring and real-time imaging of alkaline pH and viscosity in living cells. *Microchem. J.* **2022**, *173*, 107010.
(104) Su, P.; Wen, L.; Yan, J.; Zheng, K.; Zhang, N. Baso-chromic spiropyrrolizine: The spiromerocyanine isomerization and alkaline detection. *J. Mol. Struct.* **2022**, *1250*, 131631.
(105) Jiang, T.; Wang, X.; Wang, G.; Wang, Y.; Wang, K.; Xuan, X.; Chen, C.; Jiang, K.; Zhang, H. Light-activated "cycle-reversible intramolecular charge transfer" fluorescent probe: monitoring of pHi trace change induced by UV light in programmed cell death. *Chem. Commun.* **2019**, *55*, 5279−5282.

https://doi.org/10.1021/acsomega.2c04969
ACS Omega 2022, 7, 36988−37007